PAP-193

PAP-193

PAP-193

TT 75-53099

Genehmigte Dissertation zur Erlangung des
Akademischen Grades eines Doktor-Ingenieurs
von der Fakultaet fuer Bauwesen der Technischen
Hochschule Karlsruhe, Feb. 1964.

Henry T. Falvey

ENERGY LOSSES AND FLOW CONDITIONS IN GATE SLOTS
(Energieverluste und stroemungevorgaenge
bei nischen).

Translated from German

Prepared for the Bureau of Reclamation, U. S.
Department of the Interior and National Science
Foundation, Washington, D.C. by Saad Publications
(Translations Division). Translation reviewed
and corrected by H. T. Falvey.

1975

TT 75-53099

ENERGY LOSSES AND FLOW CONDITIONS IN GATE SLOTS

Dissertation presented in fulfillment of the
requirement of the academic degree of
DOCTOR-ENGINEERS
of the Faculty of Civil Engineering
Technical University Karlsruhe

by

Master of Science Henry T. Falvey
from Denver, Colorado, USA

Day of viva voce: 28 February 1964
Examiner : Professor Dr. Ing. Dr.Ing.E.h.P. Boss
Co-Examiner : Professor Dr. Ing.E.h.Dr.Ing.H.Wittmann

Foreword

Gate slots are frequently installed to support stop logs and gates which isolate turbines of powerhouses from water during repairs. The energy loss due to slots and the flow conditions in the slots have so far been investigated to a very small extent, yet repeated inquiries showed that there was considerable interest in this problem.

In the present work an attempt is made to analyze flow conditions in the slots and develop a process to determine the losses due to slots.

The investigations were made possible with the facilities, instruments and auxiliary services of the Institute of Hydromechanics Dams and Water Supply of Technical University, Karlsruhe. I am grateful to my mentor Dr.Ing. Dr. Ing.E.h.P. Boss for stimulating this work, for his keen interest and great support in research work.

Karlsruhe, March 1964.

Henry T. Falvey

Literature

[1] Mosonyi, Wasserkraftwerke, (Water-power stations) Vol. 1, Hungarian Academy of Sciences Press 1956.

[2] Wickert, Hydrodynamische Probleme im Stahlwasserbau (Hydrodynamic problems in steel water structure), VDI Zeitschrift, Vol. 105, No. 3, 1963.

[3] Ball, Hydrodynamic characteristics of Gate Slots, ASCE Proc 85 Hy 10, n 2224, October 1959.

[4] Schalnew, Kavitation von Schutznischen (Kavitacija scitovych pazov) Izv. Akad, Nauk. SSSR, Old. techn. Nauk, Mech i Masino-Stroenie, Moskva, Nr 2, 14 Lit.

[5] Schlichting, Grenzschicht - Theorie, (Boundary Layer Theory), Verlag G. Braun, Karlsruhe.

[6] Schlichting, Laminare Kanaleinlaufstromung (Laminar Canal Inlet Flow), ZAMM 14m 1934.

[7] Schiller, Untersuchungen uber laminare und turbulente Stromung (Studies on laminare and turbulent flow), VDI Forschungsheft 248, 1922.

[8] Szablewski, Der Einlauf einer turbulenten Rohrstromung (The Inlet of Turbulent Pipe Flow), Ingenieur-Archiv 21, 1953.

[9] Robertson-Bennett, Discussion of Hydraulic Characteristics of Gate Slots, ASCE Proc 86 Hy 5, May 1960.

[10] Nikuradse, Gesetzmass igkeiten der turbulenten Stromung in glatten Rohron, (Laws of turbulent flow in smooth pipes) VDI Forschungsheft 356, 1932.

[11] Streeter, Friction Resistance in Artificially Roughened Pipes, Trans ASCE, v. 101, 1936.

[12] Wieghardt-Tillmann, Erhohung des turbulenten Reibungwider standes durch Oberflachenstorungen - Neue Widerstandsmessungen an Oberflachenstorungen in der turbulenten Reibungsschicht, (Increase in turbulent frictional resistance due to surface disturbances - New resistance measurements in turbulent friction layer) Forschungsheft fur Schifftechnik 1, 1953.

[13] Boss, Unveroffentlichte Versuchsberichte des Institutes fur Hydromechanik, Stauanlagen und Wasserversorgung, Technische Hoohsehule, Karlsruhe. (Unpublished experimental reports of the Institute of Hydromechanics, Reservoirs and water Supply, Technical University, Karlsruhe.

[14] Kartenbeck, Ahnlichkeitsbedingungen bei Stromungs vorgangen und ihre Uberprufung durch Modellversuche, (Similarity conditions in flow processes and their testing by model experiments), Der Bauingenieur 17, 1936, No. 7/8.

[15] Abramovich, The Theory of Turbulent Jets, The MIT Press, Cambridge, Mass. 1963, pp 625-628.

Most important literature references are emphasized in text by square brackets.

b	= Width of experimental conduit	m
d	= Conduit diameter	cm
g	= Acceleration due to gravity	m/s^2
h	= Height of cross section	m
h_L	= Magnitude of energy loss	m
h_w	= Head on weir crest	
p	= Local pressure head	kp/m^2
p_o	= Reference pressure head	kp/m^2
r_o	= Pipe radius	cm
k	= Sand grain roughness	mm
t	= Slot depth	m
v	= Local velocity	m/s
v_1	= Velocity on pipe axis	cm/s
V	= Mean speed	m/s
v_*	= Shear velocity	cm/s
w	= Height of weir crest	cm
x_1y	= Flow coordinates	m
z	= $\kappa . v_1/v_*$	1
c_p	= Pressure coefficient	1
c_w	= Resistance of coefficient	1
E_{kin}	= Total kinetic energy	kp.m
E'_{kin}	= Total kinetic energy with respect to mean velocity	kp.m
F	= Area	m^2
G	= Weight	kp
H	= Total energy line	m
K	= Resistance	kp
K_N	= Slot loss coefficient	1
K_N	= Slot loss coefficient with w/b = 1.00	1
K_p	= Pitot tube coefficient	1
L	= Length ratio factor	1
Q	= Discharge	m^3/s
R	= Hydraulic radius	m
R	= Reynold's number	1
U	= Wetted perimeter	m
W	= Slot length	m
α	= Kinetic energy correction factor	a
γ	= Specific gravity	kp/m^3
δ	= Boundary layer thickness	cm
λ	= Local pressure loss coefficient	1
$\bar{\lambda}$	= Total loss coefficient	1
ρ	= Density	$kp.s^2/m^4$
μ_k	= Contraction coefficient	1
μ_w	= Weir coefficient	1
κ	= Velocity profile factor	1
τ	= Wall stress, stress	kp/m^2
ν	= Kinematic viscosity	m^2/s

Dimensions other than those given here are explained in text.

I. Introduction

From the ideal point of view all flow surfaces in hydraulic installations should be steamlined. This ideal state, however, cannot be realized in many fields of practical application. An example for which a deviation from this ideal case is necessary, is that of the construction of slots in flow channels for removing and retaining gates and emergency closures; e.g., stop logs.

In low-pressure installations like weir power stations, the slots normally serve as supports for gates in order to keep the power station dry during repairs of the turbines (fig. 1).

Abb. 1. Typische Wehrkraftanlage

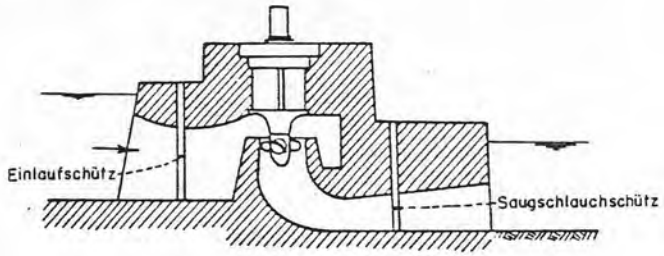

Figure 1. - Typical weir power station.
Key: 1. Inlet gate
2. Draft tube gate

In normal operation the energy loss caused by these slots need not be taken into consideration. If, however, the efficiency of the turbines is to be determined, this energy loss has to be taken into account. Mosonyi [1] has developed an equation to determine the magnitude of the energy loss due to the slots. This equation is based upon the assumption that the energy loss occurs due to expanding of water on entry into the slot and acceleration of water on exit from the slot. In order to determine the magnitude of these losses, the Momentum equation for expansion losses which was derived by Borda would be used; for contraction loss in the inlets the contraction coefficients determined by Wiesbach would be used.

These considerations take account of the fact that different eddies are formed in slots of different dimensions and so the expansion of water in the slot and hence the losses are also affected. As shown later, these dimensions have a significant effect upon the losses.

Even for medium and high pressure installations slots are used as supports gates; e.g., sliding sluices and rolling vertical lift gates which are used for water pressures of over 100 m.

In such installations not only the energy losses due to slots have to be taken into account; the danger of cavitation as well as damage of hoisting chains for the gates due to turbulence in the slots must be considered.

Abb. 2. Rollschütz Haltevorrichtung [3]

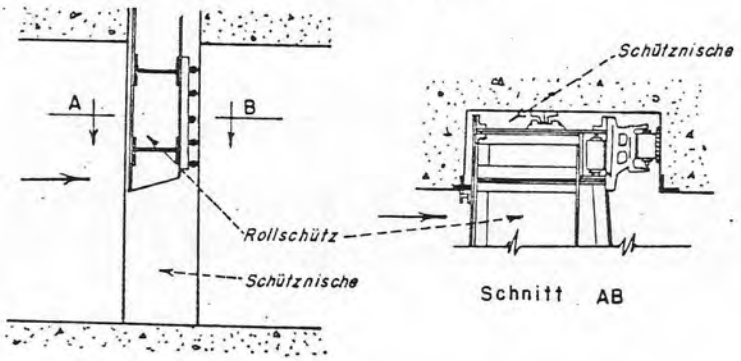

Figure 2. - Rolling anchoring system. Vertical left gate.
Key: 1. Roller gate
2. Gate slot
3. Gate slot

Cavitation and pressure distribution in the slots have been very exhaustively investigated [2], [3], [4]. On determination of energy losses due to slots, however, there are few publications in the technical literature and only a meager amount of information regarding flow conditions in the slots.

The subject of this work is limited to the investigation of energy losses caused by various shapes and dimensions of slots. The flow conditions in slots and their effect upon energy loss are also described.

Knowledge about following points was obtained during this study:

A. Effect of the slots on the increase of boundary-layer thickness and velocity distribution.

B. Form of the flow distribution in the slots for various slot configurations.

C. Effect of flow distribution in the slots upon the slot loss coefficients

D. Determination of slot loss coefficient for arbitrary rectangular slot-dimensions with the help of semi-empirical curves

E. Effect of the variations of the rectangular slot form upon the slot loss coefficient

II. Hydraulic Principles of Pipeflow

A. Inlet flow

Schlichting [5] has defined pipe-inlet flow as state of stationary flow present at the inlet of the pipe. The velocity profile is rectangular at the inlet cross section. This profile gradually varies downstream, due to friction effects, up to a certain distance from the inlet; thereafter, there is no additional profile change. Since this change of profile which corresponds to the growth of a boundary layer occurs in a pressure gradient, the equations developed for boundary layer thickness along a plate or a level wall cannot be used. Since, moreover, the local velocity does not remain constant downstream from the pipe inlet, the equations for fully developed pipe flow are also not applicable. Even though a general solution for inlet flow has not been found so far, various research workers have succeeded in obtaining solutions for special cases; e.g., for laminar channel inlet flow and laminar pipe inlet flow as well as turbulent pipe inlet flow [6], [7], and [8].

Abb. 3. Druckverteilung am Ende der Nische [9]

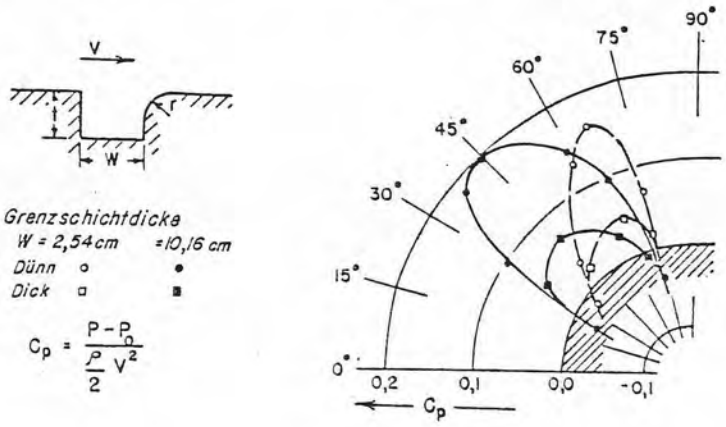

Figure 3. - Pressure-distribution at the end of the slot [9].

Consideration of the inlet flow is important for two reasons. First of all the gates, and hence the slots, are frequently found in places where inlet flows are present; e.g., the case in weir power stations and emergency gates which are located at inlets to pressure conduits and outlet works.

The second reason for this is that the magnitude of pressure distribution at the end of slot due to the growth of relative boundary layer thickness is reduced (fig. 3). Hence, one may conclude that the strength of circulation in the slot or the turbulence in the slot with a thick boundary layer would be small. Moreover, it is expected that the energy loss in thick boundary layers becomes small due to reduced turbulence (c.f. section II.3.b., also). Hence, in experiments with thin boundary layers in pipe inlet, the eddy formation in the slot would be most vigorous and the loss attributable to the slot would be maximum.

1. Turbulent inlet flow for pipes with circular cross section

The flow processes in laminar inlet flow have been very thoroughly studied. On the other hand, very little is known about turbulent inlet flow. This problem has been mathematically elucidated by Szablewski [8], but there is no experimental proof of his equations in the inlet section. When these equations are applied to the region of developed flow, there is a good agreement with the experimentally determined values.

Szablewski, in his studies, has started with the assumption that a turbulent boundary layer is present downstream from the initial cross section (fig. 4). He also assumes that the coefficients K and $V_* \delta_0 / \nu$ are constant and independent of pressure gradient and Reynolds' number $R = Vd/\nu$. Substitution of values $K = 0.42$ and $V_* \delta_0 / \nu = 7.01$ from the Nikuradse measurements [10] gives the combination of velocity distribution of inlet flow on the developed pipe flow.

Abb. 4. Einlaufströmung in ein Rohr [8]

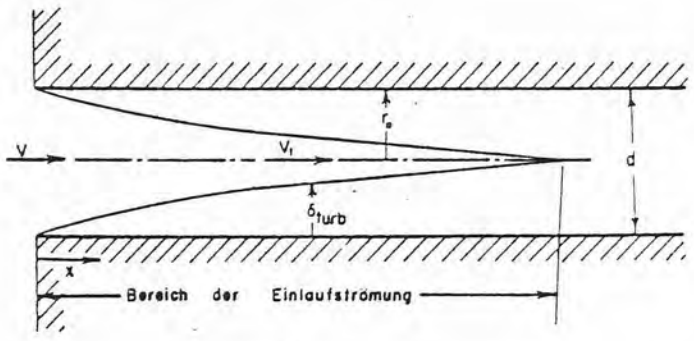

Figure 4. - Inlet flow in a tube [8].

Using the logarithmic velocity theorem:

$$\frac{u}{v_*} = \frac{1}{\kappa} \ln \frac{y v_*}{\nu} - \frac{1}{\kappa} \ln \beta$$

and the continuity theorem, one obtains equations for the velocity on pipe axis (v_1/v) and for the relative boundary layer thickness (δ/r_o) as explict functions of z, where $z = \kappa v_1/v_*$ is a function of x/r_o. Using the theorem of momentum, the local loss coefficient

$$\lambda = \frac{dp/dx \cdot d}{\rho/2 \cdot V^2}$$

and the total loss coefficient

$$\bar{\lambda} = \int_0^{x/d} \lambda d\,(x/d)$$

are obtained as explicit functions of z. The relationship between z and x/r_o is given by an integral which can be solved to an approximation. The hydraulic characteristics of flow as function of x/d instead of x are shown in figures 5 to 8.

Abb. 5. Örtlicher Druckverlust [8]

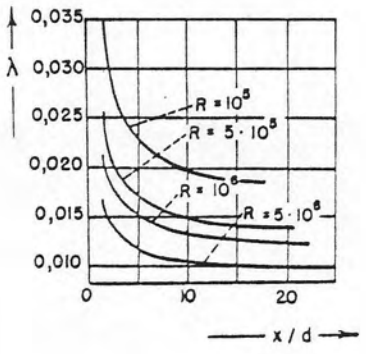

Figure 5. - Local pressure loss.

Abb. 6. Gesamtdruckverlust [8]

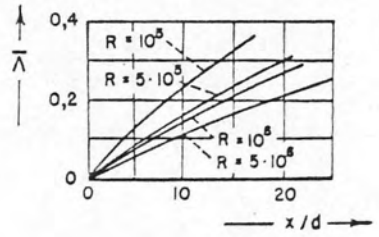

Figure 6. - Total pressure loss.

Abb. 7. Geschwindigkeit in Rohrachse [8]

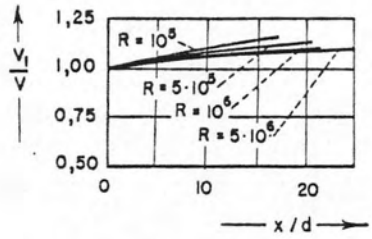

Figure 7. - Velocity on pipe axis.

Abb. 8. Grenzschichtdicke [8]

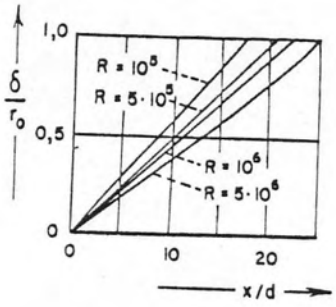

Figure 8. - Boundary layer thickness.

2. Turbulent inlet flow for pipes with noncircular cross sections

The problems of turbulent flow in pipes with noncircular cross sections has been investigated for developed pipe flows [5]. As far as could be found, there is no literature available which treats the inlet flow for noncircular cross sections. From the investigation of developed pipe flow along with the results of the previous section, one can draw conclusions regarding flow processes in the inlet section of pipes with a square cross section.

A particularly notable characteristic of the developed pipe flow in pipes with rectangular cross section is the relatively large velocity in the corners. These high velocities may be explained, according to Schlichting [5], by the presence of a secondary motion by which the flow occurs along the angle bisectors in the corners. The impulse due to the secondary motion is the reason of high velocities in the corners (fig. 9).

The velocity distribution in a noncircular cross section introduces a new unknown factor in calculation. In a circular cross section a tangential stress on the wall [$\tau_0 = f(dv/dy)$] can be assumed constant at all points of the surrounding space, because the velocity profile is axially symmetrical. In a noncircular cross section, however, one cannot assert that τ_0 is constant at all points of the entire surrounding spaces since dv/dy is not constant at all points. Actually, it may be assumed that τ_0 in the corners is less than in the middle of two corners. Although there certainly are relationships between tangential stress on the wall and secondary flow, the present knowledge of this complicated flow behavior is not sufficient to explain these relationships.

Abb. 9. Isotachenbilder für Rohre von nichtkreisförmigem Querschnitt [5]

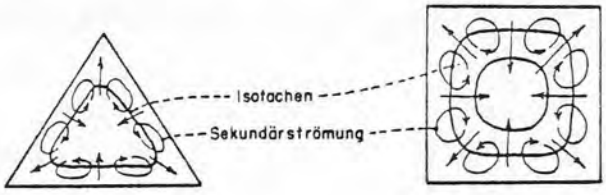

Figure 9. - Isotachs for pipes with noncircular cross section [5].

The local loss coefficient for developed pipe flow in noncircular cross sections is usually measured with respect to the hydraulic radius R_h where:

$$R_h = F/U$$

(F = cross sectional area, U = wetted perimeter)

In a circular cross section, the diameter is equal to four times the hydraulic radius. Hence the resistance formula, which is normally derived with respect to diameter, is:

$$\frac{p_1-p_2}{L} = \frac{\lambda}{d} \cdot \frac{\rho}{2} \cdot v^2 = \frac{\lambda}{4 \cdot R_h} \cdot \frac{\rho}{2} v^2 = \frac{\lambda \cdot \rho \cdot v^2}{8 \cdot R_h}$$

Abb. 10. Widerstandsgesetz für glatte Rohre [5]

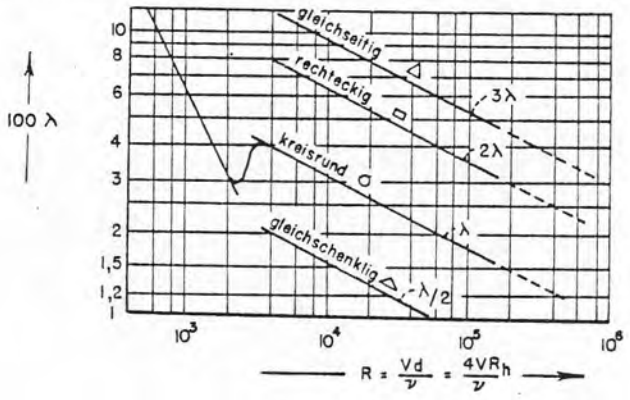

Figure 10. - Resistance formula for smooth pipes [5].

Figure 10 shows the local loss coefficients for some cross sections. The individual ordinate values are multiplied with 3, 2, and 1/2, respectively, since otherwise the curves would overlap.

Comparison of the characteristics of developed flow in noncircular cross sections with those of inlet flow of the previous section leads to the following conclusions:

Due to secondary flow, the velocity profile and boundary layer thickness are not the same as in circular flow. Due to lack of knowledge of secondary flow, however, no evaluation of the relative boundary layer thickness and the lengths of inlet section is possible.

The cross sectional shape has only a small influence on the loss coefficient curve. Thus the local loss curves and the total loss curves which apply to circular pipes can be applied with a good approximation to the inlet flow in noncircular cross sections.

B. The kinetic energy of pipe flow

For the flow, a pipe the weight (of water) dG, flowing through every element of area dF of the cross section per second, is given by the formula:

$$dG = u \cdot \gamma \cdot dF$$

The kinetic energy of the mass is:

$$dE = 1/2 \cdot u^2/g \cdot dG = \rho/2 \cdot u^3 \cdot dF$$

Hence the total kinetic energy in the cross section is given by:

$$E = \int_F \rho/2 \cdot u^3 \cdot dF$$

Inserting a constant mean velocity V in the expression, one obtains:

$$E' = \frac{FV^3}{2} \cdot \rho$$

If u is not constant over the cross section then $E > E'$. In order to obtain the actual kinetic energy in the cross section, E' must be multiplied with a correction factor α, where $E = \alpha E'$.

If velocity distribution is constant, the correction term is obtained from:

$$\alpha = \frac{E}{E'} = \frac{1}{F}\int_F (u/V)^3 \cdot dF$$

In those cases where the velocity distribution is unknown the correction term is best determined graphically.

Introducing the correction term in Bernoulli's equation for straight pipe flow in which static pressure at all points of the cross section is constant, the equation assumes the form:

$$\alpha \frac{V^2}{2g} + \frac{p}{\gamma} = \text{constant}$$

C. Flow resistance

The resistance offered by a body to flow is equal to the resultant force, acting in the direction of flow, of all tangential stresses and all normal pressures which act upon the surface of the body. In streamlined bodies this force is produced by tangential stress alone because without separation the pressures in front of and behind the body are equal. With fully developed pipe flow the force is similarly produced by tangential stress alone. For nonstreamlined bodies (e.g., a circular plate perpendicular to the direction of flow) the force due to stress is negligible as compared to the normal pressure produced by separation. The resistance which only is due to tangential stress is called frictional resistance, while that due to normal pressure is called form resistance. Between these two extremes, the flow depends upon the geometrical shape of the body and the Reynold's number because both tangential stress and normal pressure forces are significant. Flow around a sphere is an example of this.

1. Surface resistance

Resistance in pipes has been investigated in detail by Nikuradse and Prandtl. Two very important equations produced by their studies are: the universal resistance theorem for smooth pipes:

$$\frac{1}{\sqrt{\lambda}} = 2.0 \text{ Log } \frac{Vd}{\nu}\sqrt{\lambda} - 0.8$$

and the resistance theorem of fully developed rough flow:

$$\frac{1}{\sqrt{\lambda}} = 2.0 \text{ Log } \frac{d}{k_s} + 1.14$$

in which k_s is the grain size of the Nikuradse sand-roughness parameter. For the transition of "hydraulically smooth" to "fully rough" one can use the formula of Colebrooke and White:

$$\frac{1}{\sqrt{\lambda}} = 1.74 - 2.0 \text{ Log } \left(\frac{k_s}{r} + \frac{18.7}{R\sqrt{\lambda}}\right)$$

In general, artificial as well as natural roughness can be expressed as equivalent sand roughness. An example in point is the experiment of Streeter [11] in which the inner walls of the pipe had spiral threads. Some of the thread forms studied were rectaugular and thus form a similarity with the gate slots. Since the spiral threads are comparatively small, they chiefly affect the tangential stress and, therefore, can be expressed as values of sand roughness (table 1).

Table 1. -

Roughness		Radius, inches	Sand roughness, inches	Depth of thread, inches	No. of threads per inch
II	0.0266	1.034	0.0066	0.005	23
III	0.0272	1.035	0.0072	0.005	23
IV	0.0465	1.043	0.0370	0.012	23
VII	0.0700	1.052	0.1005	0.022	11.5

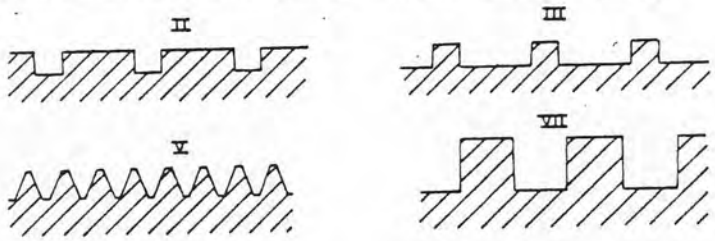

2. Form resistance

The energy losses due to form resistance cannot be determined analytically, but experimentally. The sudden expansion of cross section is an exception in which the results obtained by analytical methods agree very well with experimentally obtained values (fig. 11).

Equating the pressure force and the impulse difference between 1 and 2 (fig. above) and neglecting the tangential stress on wall, one gets:

$$p_1F_1 + p_1 (F_2 - F_1) - p_2F_2 = Q \cdot \rho \cdot (V_2 - V_1)$$

If the loss term is taken into consideration in the Bernoulli's theorem between 1 and 2, one gets:

$$P_1/\gamma + V_1^2/2g = p_2/\gamma + V_2^2/2g + h_L$$

solving these two equations for h_L, with $Q = V_1F_1 = V_2F_2$

$$h_L = \left[1 - \frac{F_1}{F_2}\right]^2 \cdot \frac{V_1^2}{2g} = K \frac{V_1^2}{2g}$$

This is known as Borda's expansion loss.

Abb. 11. Unstetige Querschnittserweiterung

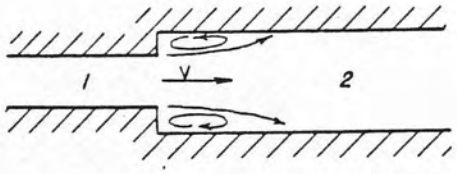

Figure 11. - Sudden expansion.

Another problem which can be solved by semiempirical methods, is the sudden contraction of cross section (fig. 12).

Assuming that the loss in accelerated flow would be very small as compared to that of the decelerating flow, the loss between 2 and 0 may be ignored. Energy loss between 0 and 1 is then the total loss due to the contraction. It follows from the above equation that:

$$h_L = \frac{(V_0 - V_1)^2}{2g}$$

The area of the contracted flow at 0 is expressed by a contraction coefficient C_k; this is defined as:

$$C_k = F_0/F_1$$

Through consideration of the continuity theorem:

$$Q = V_0 \cdot C_k \cdot F_1 = V_1 \cdot F_1$$

one obtains the following expression for the loss:

$$H_L = \left[\frac{1}{C_k} - 1\right]^2 \cdot \frac{V_1^2}{2g}$$

The values for C_k are experimentally determined; e.g., by Wiesbach with:

$$C_k = 0.63 + 0.37 \cdot F_1 F_2$$

Abb. 12. Unstetige Rohrverengung

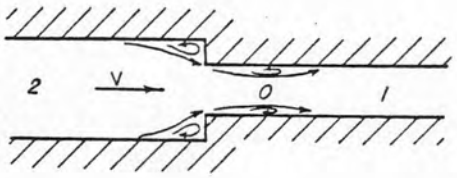

Figure 12. - Sudden contraction.

3. Isolated roughness

In general, the resistance due to single roughness generally consists of form resistance and surface resistance. Surface resistance is created because the velocity profile and, hence, the tangential stress, varies in the neighborhood of the roughness.

Abb. 13. Widerstandsbeiwert für rechteckige spaltförmige Löcher [12]

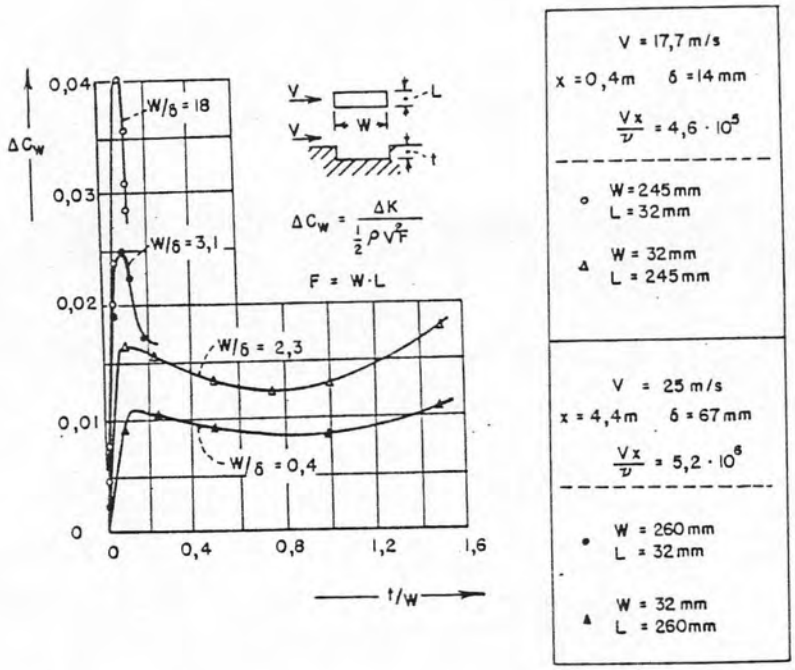

Figure 13. - Coefficient of resistance for rectangular crack-shaped holes [12].

The resistance for a large number of individual roughness has been experimentally investigated by Wieghardt [12]. Experiments were carried out in a wind tunnel of rectangular cross section. Resistance was measured by weighing a rectangular measuring plate, which was kept movable in a notch of the lower wall of the wind tunnel. The difference of the resistance of measuring plate with and without roughness gave the desired additional resistance. Among the roughness forms investigated by Wieghardt, there were also right angle crack-like holes of rectangular shape, resembling slots (fig. 13). A particular property of these curves is unusually large loss at a ratio $t/w \approx 0.125$ and the comparatively small loss at $t/w > 0.125$ for large values of w/δ. This phenomenon is explained by vortices, which are formed in the holes and lead to the various resistances (comp. III 3 c).

III. Model Experiments

A. The model

In order to investigate the energy loss and flow processed in the slots, an experimental pipe of 357 cm length with a square cross section and having 12.0 cm long sides was made with a smooth finish concrete (fig. 14). In order to have a uniform inflow in the experimental pipe, a bell-mouth inlet section (e), corresponding to the equation:

$$(x/b)^2 + (4y/b)^2 = 1$$

in which b is the length of side, was used (fig. 15). The slots were located opposite to each other on the side walls and were in a specially made section 50 cm downstream from the inlet (fig. 16). The maximum length of the slot was 23.85 cm and maximum depth was 12.20 cm. The walls (w) of the specially made section, in which the slots (n) were placed, was made of concrete. The cover was made of 12-mm-thick plexiglass plate and fixed by screws (s). Hence, the cover was easily removed whenever a change in the slot dimensions was to be made. A pitot tube (pt) used for measuring the velocity profile in the pipe was inserted through a hole in the cover. Five pressure connections (ds) were inserted in each wall of the special section to determine the static pressure head in the experimental cross section. The bottom of the special section consisted of a glass plate (g) which was formed into the walls. The transparent bottom and the lid allowed an observation of flow conditions in the slots. A measuring point 320.0 cm downstream from the start of the pipe was provided to determine the energy loss due to the slots. At this measuring point, a portion of concrete cover of the experimental pipe was replaced by a removable plexiglass cover (pd) (fig. 17). Five pressure connections in each wall and another five (ds) in the bottom were installed in the experimental pipe in order to determine the static pressure head in the measurement cross section.

The water for the model was taken from the laboratory circulation system (fig. 18). In this system the water from a sump was pumped into a reservoir. Water level in the latter was kept essentially constant by means of

a funnel-shaped weir (t). Water from the reservoir was brought to an intermediate tank vessel and led to the model through a pipe (g) and, after circulation through the model, was led back to the sump. The amount of water was controlled by a valve in the supply pipe. By this system a stationary flow was obtained in the model after about 10 minutes and kept constant throughout the experiment.

B. Measurement system

1. Discharge

The discharge flowing in the model is determined by a sharp-edged rectangular weir without side contraction (fig. 15). Under conditions of free overflow the discharge can be determined with the help of the following equation:

$$Q = \mu \cdot \frac{2}{3} \cdot b \cdot \sqrt{2g} \cdot h_w^{3/2}$$

Abb. 14. Gesamtmodellanlage

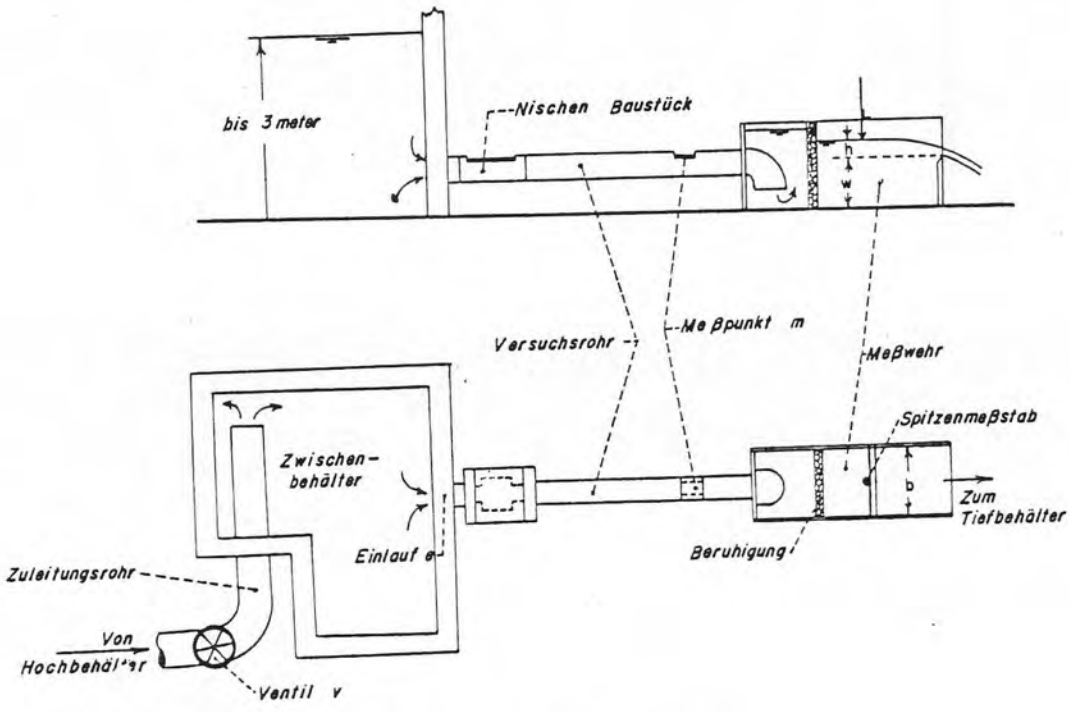

Figure 14. - The model (overall view).

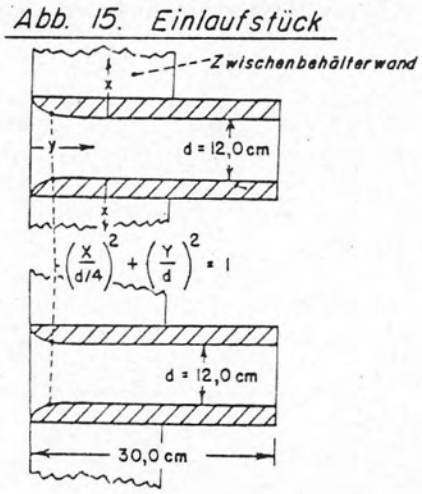

Figure 15. - Inlet section.

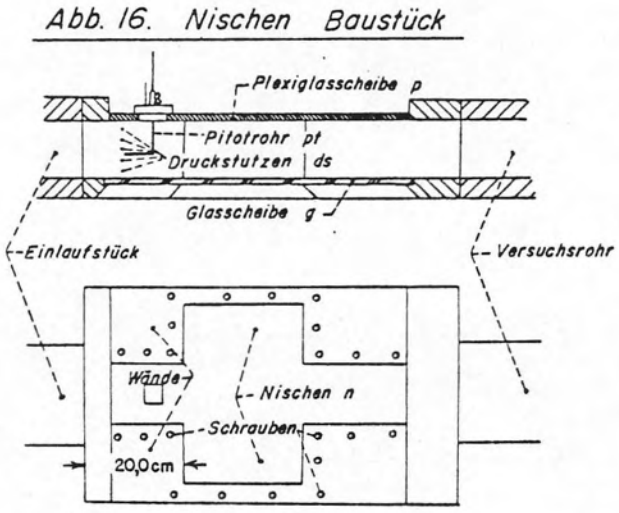

Figure 16. - Slot section.

Abb. 17. Meßpunkt m

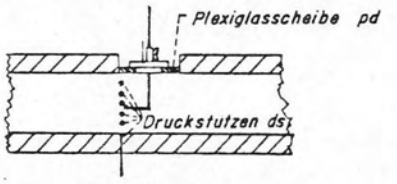

Figure 17. - Measuring point m.

Abb. 18. Kreislaufsystem des Laboratoriums (Schema)

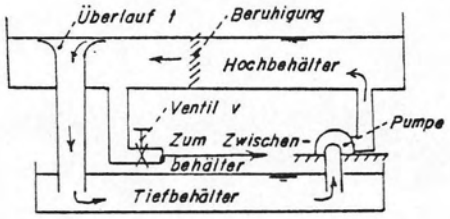

Figure 18. - Circulating system of the laboratory (schematic).

in which b = width of the weir = 75.15 cm; h_w = head of water over the weir crest. μ = weir coefficient.

The weir coefficient is determined by the formula of Rehbock:

$$\mu = 0.605 + 0.08 \frac{h_w}{w} + \frac{1}{1000\ h_w}$$

in which w = height of weir crest; the height of weir crest of the model amounted to w = 60.0 cm.

2. Static pressure measurements

Static pressure p/γ is measured with piezometer taps consisting of copper tubes with external diameter of 4.0 mm and internal diameter of 2.0 mm. Five pressure connections were installed 2 cm from each other in a row on both walls in the measurement cross section 12 cm upstream of the slots. The same arrangement is made in the measurement cross-section m (fig. 14) in which an additional series of five pressure connections were inserted on the floor. In order to take an eror-free reading of static pressure, the connections were filed even with the wall or, as the case may be, with the bottom, and the burrs were removed with a drill of 2.0 mm diameter. A comparison between the respective pressure connections showed a maximum pressure difference of ! 0.6 percent. The tubes of the various pressure connections were then joined to a single tube leading to a manometer which read the static pressure.

3. Velocity measurements

Measurements of local velocity were taken from the difference of the pressure head readings in the pitot tube and static pressure of the pressure connections. This difference gives the dynamic pressure head (h) where:

$$h = \frac{u^2}{2g}$$

According to Bernoulli's theorem, the velocity can be calculated from the equation:

$$u = 0.443 \cdot K_p \cdot \sqrt{h'}$$

where u is velocity in m/s, h^1 is the dynamic pressure head in cm and K_p is the pitot tube coefficients.

The amount of water flowing is obtained by graphic integration of the local velocity over the surface according to the formula:

$$Q = \int_F u \cdot dF$$

A comparison of this amount of flow with the amount of flow from the weir gives the basis of a calculation of K_p. K_p was found to be 0.985 from the mean of seven separate amounts of flow between 32 and 80 L/s. The greatest difference between the amount of flow from weir and the graphical integration of local velocity was ±1.5 percent.

Abb. 19. Pitotrohr und Haltevorrichtung

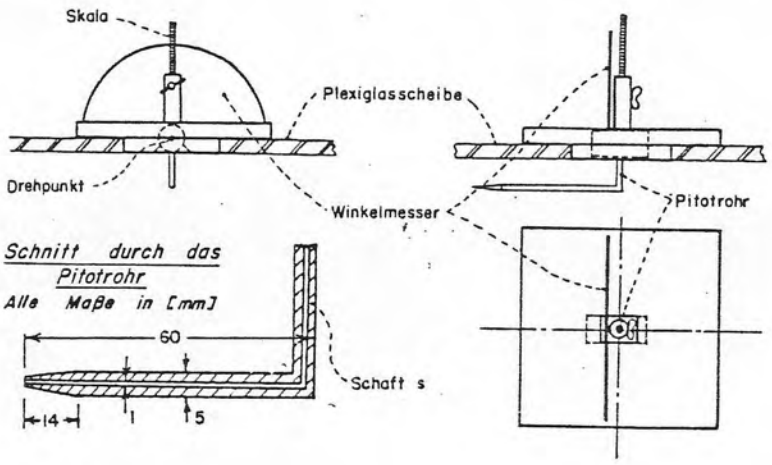

Figure 19. - Pitot tube and fixing arrangement.

The pitot tube was made from a brass tube of 5.0 mm external and 1.0 mm internal diameter (fig. 19). It could be moved in the direction of the shaft and also about a maximum angle of ±45°. Distances in the direction of the shaft could be regulated with an accuracy of ±0.2 mm and angle with an accuracy of ±0°07' with this arrangement.

4. Manometer

All pressures in the model (static pressure, pressure head and height of water level in the intermediate tank) were measured with a manometer. Glass tubes joined to measuring points with rubber tubes and vertically fixed to a measuring table were used as the manometer. Millimeter paper stuck to the board behind the glass tubes allows the water column heights to be read with an accuracy of ±0.2 mm.

C. Experiment

Investigation of the energy losses due to slots required the experiment to be done in three different steps:

1. Determination of velocity profile with and without slots in order to determine the kinetic energy-correction factor α and the boundary layer thickness δ;

2. Determination of total loss $\bar{\lambda}$ on the downstream measuring point without slots; and

3. Determination of total loss $\bar{\lambda}$ on the downstream measuring point under different slot conditions and with simultaneous observation of flow conditions in the slots.

For 1.

The velocity profile was first determined, without slots at two points with flows about 77 L/s and 31 L/s. These points were 12 cm above the slots and at the downstream measuring point. Velocities determined with flow of 77 L/s indicated that the flow was symmetrical over the entire cross section on measuring point m (fig. 20). Hence the subsequent measurements were taken only from the bottom, from one sidewall and one corner of the bottom to the centerline of the conduit. The distances for velocity measurements near the bottom and sidewall were between 1 and 2 mm. This measurement interval was increased to 5 mm towards the middle of the tube where differences in velocity are small. The distances between the measuring points and the corner varied between 5 and 10 mm.

Velocity measurements were initially taken for a slot length of w/b = 2.0 with different slot depths; t/w = 0.5, 0.25, and t/w = 0.125. The amounts of flow for these measurements were 53 L/s and 77 L/s. Measuring distances were the same as in the preceding section.

Abb. 20. Isotachenbild bei Q = 77 l/s

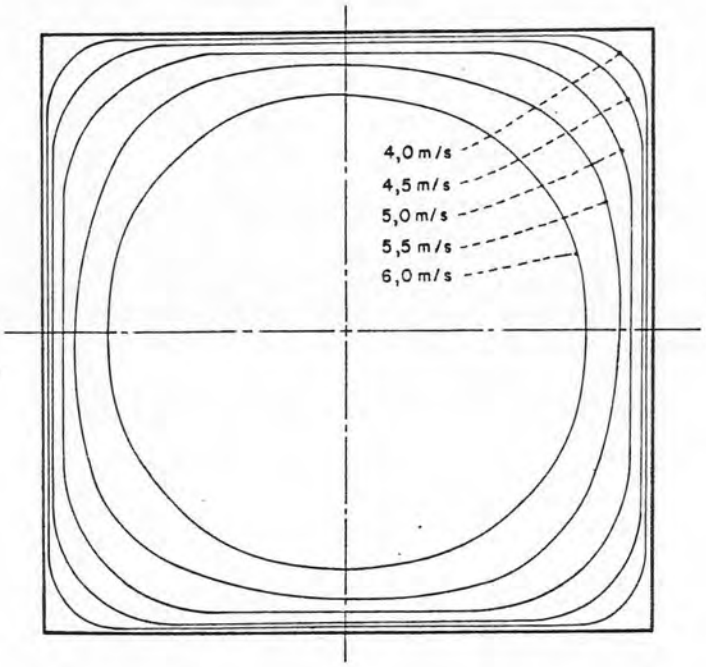

Figure 20. - Isotachs at Q 77 L/s.

For 2.

The total loss $\bar{\lambda}$ without slots on the downstream measuring point was measured for 30 different amounts of flow, so as to determine the ratio of total loss to Reynold's number. The amounts of flow were controlled by means of a valve on inlet tube leading to the model and measured with the calibrated weir (fig. 14). In order to obtain accurate mean velocity values from the amount of flow, the area of measurement cross section had to be accurately determined. This was done by direct measurement of width on the bottom, at middle height and on the cover with an inside spring caliper, and by measurement of height at a distance of 20 mm on both sides of the control line with a depth gage.

Since the kinetic viscosity in Reynold's number depends upon temperature, the water temperature in the calibrated weir was taken before and after 30 measurements.

At each new adjustment of amount of flow, a waiting time of 5 to 10 minutes was needed before a stationary flow was attained and readings could be taken. Readings were taken for the water level in the intermediate container, the static pressure head on measuring cross section, and the amount of flow.

For 3.

The total loss $\bar{\lambda}$ was determined at three different slot lengths (w/b = 2.0, 1.0, and 0.5) and various slot depths at each length. In addition to the rectangular slots, a slot with downstream sloping and elliptic edges and another with built-in piece were also used since these shapes are found in practice. In general, 15 to 20 discharges were generally tested for each slot dimension. An attempt to photograph the flow process in the slots was partially successful. Flow visualization was tried by introducing nigrosin as well as air bubbles in the flow upstream of the slots. With small discharges, the nigrosin dye clearly showed eddy formation in separation zones; with larger discharges of the type used to determine total loss, a rapid diffusion occurred through the turbulence. Use of air bubbles showed that there was no diffusion during large discharges but a photograph showed no useful results. With normal illumination times, the bubbles appeared like haze which made the flow field unrecognizable; individual bubbles were visible under strobe light but the flow field was not discernible. In many cases the flow field was further complicated by three-dimensional eddy formation in the slots; for these reasons, the flow in the slots is shown diagrammatically instead of photographically.

D. Evaluation of the experiments

1. Velocity distribution and boundary layer thickness

In order to determine whether the experimentally determined velocity distribution is logarithmic within the boundary layer, the universal velocity distribution theorem was converted in the following way:

The theorem is:

$$\frac{u}{v_*} = k_1 + k_2 \cdot \text{Log} \frac{v_* y}{\nu}$$

where $k_1 = 5.5$ for hydraulically smooth pipes,

$= 8.5 - 5.75 \cdot \text{Log} \frac{k_* v_*}{\nu}$ for fully rough tubes, and

$k = 5.75$.

Solving for Log y, one gets:

$$\text{Log } y = \frac{u}{5.75\ v_*} - \frac{1}{5.75} \left(5.5 + 5.75 \text{ Log} \frac{v_*}{\nu}\right)$$

for hydraulically smooth pipes. Plotting Log y as ordinate and u as abscissa, one gets a straight line with a slope of $1/5.75\ v_*$, and for Log y = 0, one gets a velocity of:

$$u = v_* \ (5.5 + 5.75 \cdot \text{Log} \frac{v_*}{\nu})$$

A diagram of the experimentally determined points for such a case shows that the points lie on a line within a certain range of scatter and that this line corresponds to the velocity distribution theorem for hydraulically smooth pipes (fig. 21). The shear velocity v_* for the straight line was found from a preliminary evaluation of the equation:

$$u_o = v_* \cdot (5.5 + 5.75 \cdot \text{Log} \frac{v_*}{\nu})$$

In which u_o is determined by the experimental points. For these values of v_*, the slope of the lines passing through u_o and fulfilling the velocity theorem is:

$$= \frac{1}{5.75\ v_*}$$

Experimental points were taken from measurements as well as in vertical and horizontal planes passing through the axis of the experimental tube.

For this experiment, the boundary layer thickness assumed to be at a distance from the wall or floor in which the straight line of velocity distribution theorem and the line of central core (flow around the axis of the conduit where the velocity is constant) meet.

Slots used in this part of the experiment are appreciably longer than those found in practice, they increased the boundary layer thickness by about 30 percent. A notable phenomenon, easily seen from the results of figure 21, is that slots do increase the boundary layer thickness but have no effect upon velocity distribution.

A boundary layer thickness of 10 mm at Q = 76 L/s was measured in the region of the slots. This value showed a good agreement with boundary layer thickness in pipe inlet flow (see section 8).

Abb. 21. Geschwindigkeitsverteilung

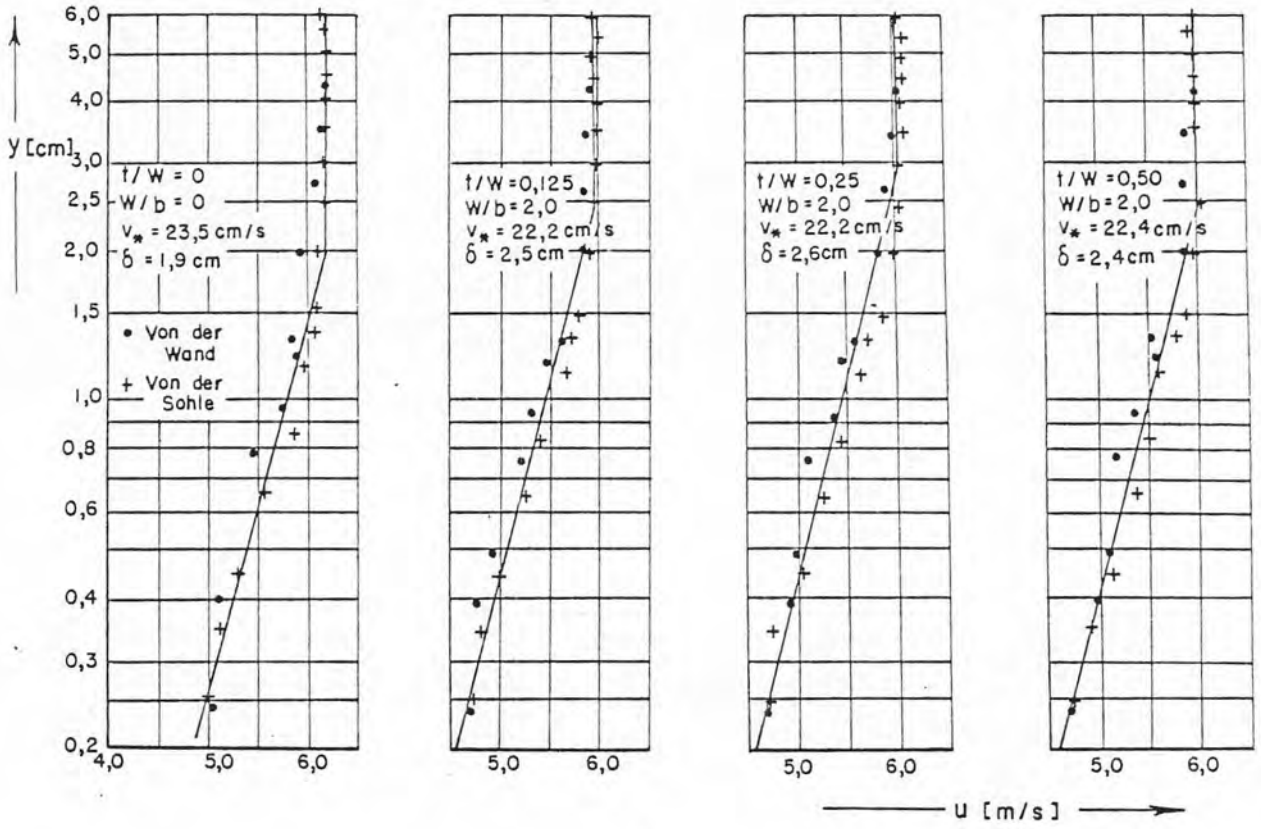

Figure 21. - Velocity distribution.

2. Loss through the slots

Energy loss produced by slots is composed of expansion loss due to widening of flow in the slots and contraction loss at exit from the slots, i.e., form resistance; energy loss due to eddy formation in the slots; and variation of boundary layer profile; i.e., surface resistance downstream of the slots.

Since it is hardly possible to separately determine these losses, a process similar to that of Wieghardt was used to determine the sum of the individual losses (cf. III 3.c). First of all the total loss without slots was determined at a point about 2.50 cm downstream from the slots (fig. 22). Then slots were made and total loss determined again. The difference between these total losses with and without the slots gave the loss due to slots only.

Since the cross section of intermediate tank is large as compared to that of experimental conduit, the velocity in intermediate tank can be neglected. Hence, Bernoulli's equation with loss term and kinetic energy correction factor is:

$$H = \frac{p}{\gamma} + \frac{\alpha V^2}{2g} + z + h_L = \frac{p}{\gamma} + \frac{\alpha V^2}{2.g} + z + \bar{\lambda}\frac{V^2}{2g}$$

Solving for total loss coefficient one gets:

$$\bar{\lambda} = \frac{H - (\alpha v^2/2g + p/\gamma + z)}{V^2/2g}$$

Before this equation can be solved, the correction factor α has to be determined since the measurement cross section is not circular and does not lie in a section in which developed pipe flow is present. The correction factor α is graphically determined as follows:

Abb. 23. Geschwindigkeit als Funktion der Fläche

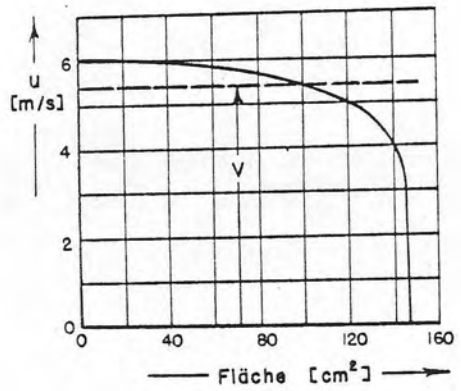

Figure 23. - Velocity as a function of area.

First of all, isotachs are plotted on a cross section diagram as shown in figure 20. The area bounded by individual isotachs is measured by a planimeter and velocity is graphically plotted as a function of area (fig. 23). Mean velocity can be obtained from this curve. Then third power of relative velocity is plotted as function of area (fig. 24). The area under this curve divided by the area of measuring cross section gives the correction factor α.

At a constant velocity over the cross section, the correction factor α is equal to 1, while for a flow in which velocity is constant over a portion of the cross section, α is greater than (1) when boundary layer thickness increases, the correction factor also increases. Study of boundary layer thickness for inlet flow showed that boundary layer thickness increased with decreasing Reynold's numbers (section II.1.a). It was also found that the boundary layer thickness increased due to the effect of the slots (section III.4.a). Hence it may be assumed that the correction factor would be large in presence of slots and increases with decreasing Reynold's numbers. Hence, it was useful to determine the correction factor for the Reynold's numbers used on this coefficient and for various slot conditions. The results of these investigations shown, in figure 25, show an experimental verification of the above considerations. The comparatively large scatter of experimental points is because the mean velocity has to be raised to third power in the determination of the correction factor. Hence, if there is a 1 percent error in the determination of mean velocity (nearly corresponding to the accuracy of planimetry), there would

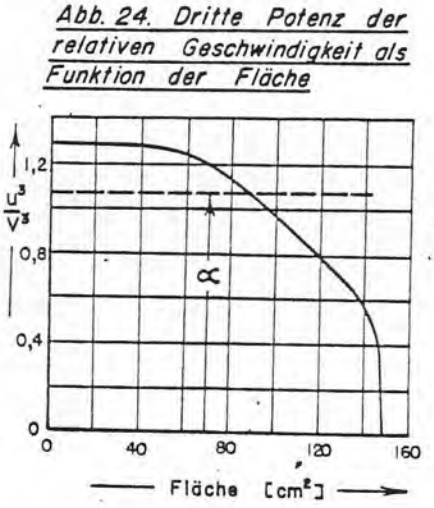

Figure 24. - Third power of relative velocity as a function of area.

be a 3 percent error in correction factor. All total losses, with and without the slots, are based upon the correction factor determined by a straight line drawn through the experimental points. It is assumed that this line is parallel to those obtained by mathematical integration of flow in a smooth pipe. Similar experiments with developed flow in a square pipe carried out in Institute of Hydromechanics, Technical University, Karlsruhe [13] yielded a correction factor of about 1.09. This factor is an approximate agreement with the results of figure 25 since the boundary layer thickness for developed flow is greater than that for inlet flow.

Abb. 25. Kinetischer Energie – Korrekturfaktor als Funktion der Reynoldsschen Zahl

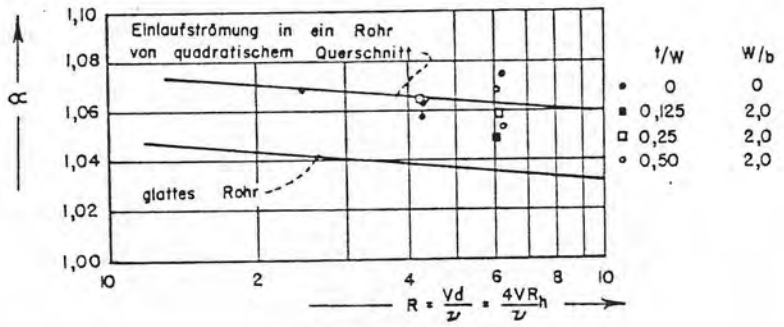

Figure 25. - Kinetic energy correction factor as a function of Reynold's number.

After the total loss for Reynold's numbers of 2×10^5 to 6×10^5 was determined, it was necessary to develop an equation for the total loss coefficient as a function of Reynold's number. For inlet flow the total loss is determined by:

$$\bar{\lambda} = \int_0^{x/d} \lambda \cdot d(x/d).$$

If the coefficient of total loss for a given cross section is considered it can be determined that for this cross section it is a function of alone. Hence,

$$\bar{\lambda}_{x/d} = \text{Constant} = f(\lambda).$$

For developed flow in smooth pipes, the coefficient of local loss as a function of Reynold's number is determined by:

$$\frac{1}{\sqrt{\bar{\lambda}}} = 2 \cdot \text{Log } R\sqrt{\bar{\lambda}} - 0.8 \text{ (Section II.3.a)}$$

If it is assumed that the local coefficient of loss in the inlet section has the same form as the loss coefficient in developed flow with the exception of constants, it is found that:

$$\frac{1}{\sqrt{\bar{\lambda}}} = A \cdot \text{Log } R\sqrt{\bar{\lambda}} + B$$

or since for a given cross section, $\bar{\lambda}$ is a function of λ alone, the equation takes the form:

$$\frac{1}{\sqrt{\bar{\lambda}}} = C \log R\sqrt{\bar{\lambda}} + D$$

The values of C and D are constant only for a given cross section without slots. With slots or with other measuring cross sections, C and D can have other values. A graphical plot of total loss coefficient recording to equation (1) with $1/\sqrt{\bar{\lambda}}$ as ordinate and $\log R\sqrt{\bar{\lambda}}$ as abscissa is shown in appendix 1 without slots and for the slot configurations studied here. The straight lines according to (2) which best correspond to the experimental points are determined by the method of least squares. From these lines the slot loss coefficient is determined by the difference in the values of total loss coefficient with and without slots, by the formula:

$$K_{slots} = \bar{\lambda}_{\text{with slots}} - \bar{\lambda}_{\text{without slots}}$$

Abb. 26. Abwandlungen der rechteckigen Nischenform

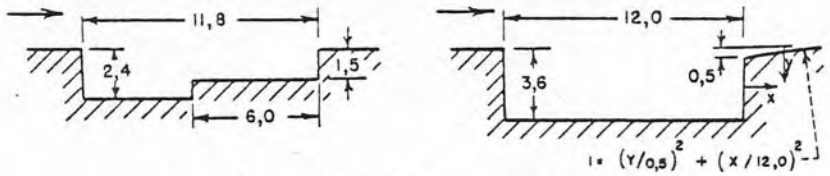

Alle Maße in [cm]

Figure 26. - Changes in rectangular shape of the slot. All measurements in cm.

The slot forms studied here were rectangular with slot length ratios of W/b = 2.0, 1.0, = 0.5. The depths varied from t/W = 0.064 up to = 1.0 for W/b = 1.0, and from t/W = 0.042 to = 0.5 for W/b = 2.0. For W/b = 0.5, only the depth ratio of t/W = 0.3 was investigated. In addition to these shapes, a slot with an insert and another one with downstream sloping and elliptically rounded edge were studied since these shapes are frequently found in practice (fig. 26).

The slot loss coefficients K_0 are shown in figure 27. The curve for W/b = 1.0 at t/W $\approx$ 0.05 to t/W = 0.5 between experimental points depends upon the shape of the curve W/b = 2.0. The curves for W/b = 1.0 and W/b = 2.0 at t/W = 0.0 to t/W $\approx$ 0.05 are based upon the sum of the losses caused by a sudden expansion followed by a sudden contraction of the conduit (see sections II.3.d and IV). All slot loss coefficients are determined with value of 5.45 for Log $R\sqrt{\lambda}$. The greatest deviation of slot loss coefficient on the basis of 5.6 and 5.2 for Log $R\sqrt{\lambda}$ was found to be $\pm$0.009.

3. Flow conditions in the slots

As already mentioned the flow process in the slots has been sketched due to difficulties faced in making the flow visible. These sketches show the general shape of flow and explain the shape of slot loss coefficient curves.

In these studies it was found that the flow conditions with the same values of t/W were similar. Moreover, a definite shape of flow is characteristic for flow conditions within a certain range of t/W. The ranges were:

a. t/W = 0 to t/W = 0.125
b. t/W = 0.125 to t/W = 0.200
c. t/W = 0.200 to t/W = 0.400
d. t/W = 0.400 to t/W = 0.500
e. t/W = 0.500 to t/W = 0.750
f. t/W = 0.750 to t/W = 1.000

For a.

When t/W is very small, the flow field is characterized by a sudden expansion which is followed by a sudden contraction. If t/W increases, the length of the flow separation zone downstream from the expansion is also greater. The limit for this lengthening was t/W = 0.125. At this ratio, a considerable contraction of the flow downstream of the slot was visible (fig. 28).

Abb. 27. Nischenverlustbeiwerte für verschiedene Nischenverhältnisse

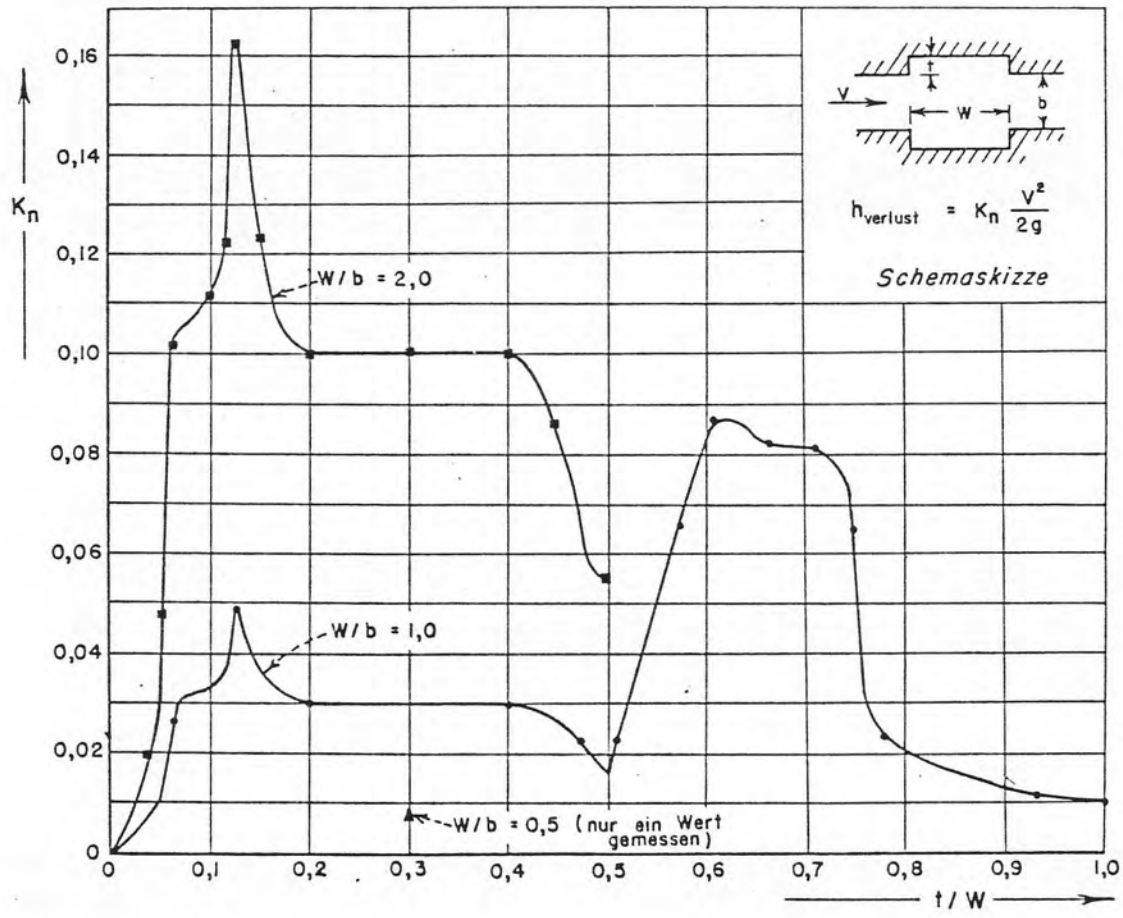

Figure 27. - Slot loss coefficient for various slot dimensions.

Abb. 28. Strömungsvorgänge in Nischen

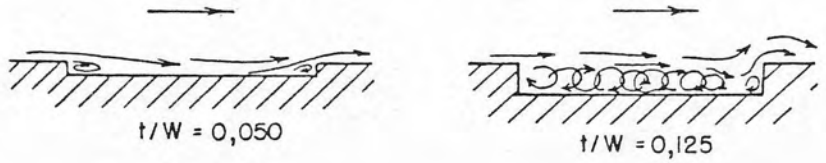

Figure 28. - Flow conditions in the slots.

For b.

If the ratio t/W becomes greater than 0.125, a nonstationary vortex is formed with horizontal axis downstream from the expansion and the contraction of the flow downstream of the slot becomes smaller (fig. 29). The sudden decrease in slot coefficient in this range at t/W may be attributed to the decrease in constriction of flow.

Abb. 29. Strömungsvorgänge in Nischen

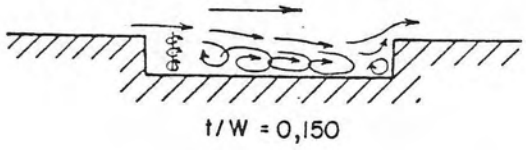

Figure 29. - Flow conditions in the slot.

For c.

Between t/W = 0.20 and t/W = 0.40, a vortex with horizontal axis is formed directly downstream from the expansion and a large vertical vortex formed upstream from the slot. In this range of t/W, the vortex conditions remain basically unchanged. This explains the comparatively constant slot loss coefficients (fig. 30).

Abb. 30. Strömungsvorgänge in Nischen

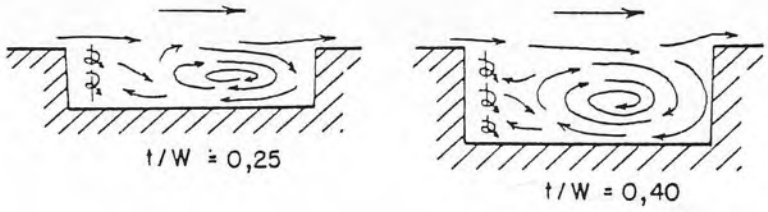

Figure 30. - Flow condition in the slots.

For d.

As t/W becomes greater than 0.40, the vertical vortex more and more filled up the slot until at t/W = 0.50, a vertical vortex or a roller was present in the slot. At t/W = 0.50, the constriction of flow downstream of the slot was very small, so that the very small slot loss coefficient in this range is explained (fig. 31).

Abb. 31. Strömungsvorgänge in Nischen

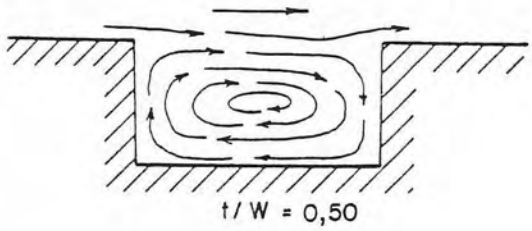

Figure 31. - Flow condition in the slots.

For e.

In the region of t/W = 0.50 and t/W = 0.75 there was a very strong eddy directly downstream from the cross section expansion which produced a large contraction of flow at the end of the slot. The contraction produced high values for the slot loss coefficient. Due to the strength of eddy, this range of slot dimensions is not recommended for high pressure installations (figure 32).

Abb. 32. Strömungsvorgänge in Nischen

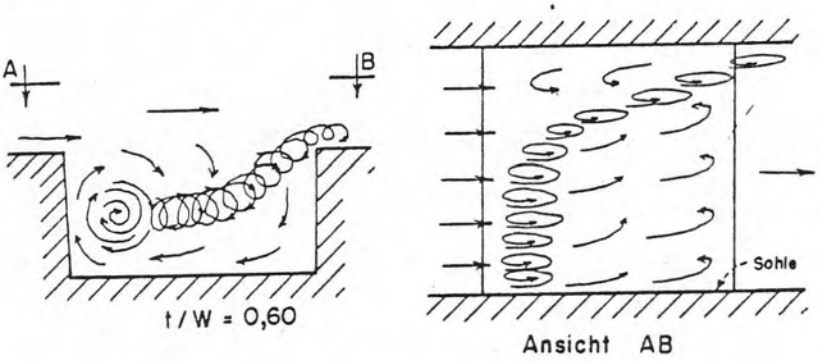

Figure 32. - Flow conditions in the slots.

For f.

When t/W becomes larger than 0.75, the strength of the vortex decreased. At t/W = 1.0, the vortex completely fills up the slots and the construction of flow downstream of the slot is very small (fig. 33). A funnel-shaped eddy is observed in the slot at t/W = 1.0.

Abb. 33. Strömungsvorgänge in Nischen

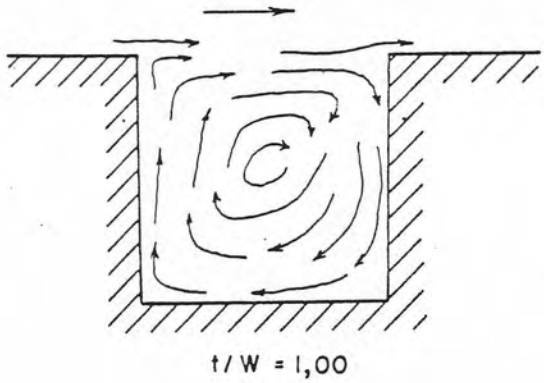

Figure 33. - Flow conditions in the slots.

IV. Determination of Slot Loss Coefficient for Arbitrary Slot Dimensions

The slot loss coefficients shown in figure 27 can be practically used for slots only when the conditions accurately correspond to those of the model. It is, however, possible to express the slot loss coefficient in a general form which holds for arbitrary slot dimensions. This general form is developed in the following sections.

The loss which is caused by a sudden expansion followed by sudden contraction is given by:

$$h_{verlust} = \left[\left(1 - \frac{F_1}{F_2} \right)^2 + \left(\frac{1}{C_k} - 1 \right)^2 \right] \frac{V^2}{2g} = K \frac{V^2}{2g}$$

Abb. 22. Feststellung des Gesamtverlustes

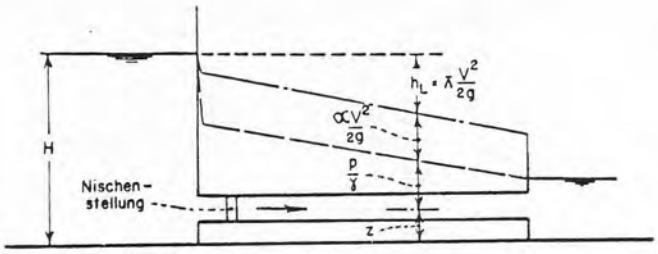

Figure 22. - Determination of total loss.

Introducing the contraction coefficients determined by Wiesbach the loss coefficient is obtained as:

$$K = \left[\left(1 - \frac{F_1}{F_2} \right)^2 + \left(\frac{0.37 - 0.37 \cdot F_1/F_2}{0.63 + 0.37 \cdot F_1/F_2} \right)^2 \right] \qquad (3)$$

The relationship between area ratio F_1/F_2 and slot ratio W/b and t/W is as follows:

It is seen from figure 34 that:

$$F_1 = b \cdot h \text{ and } F = (b + 2 \cdot t) \cdot h$$

where h is the height of cross section. This gives the area ratio as:

$$\frac{F_1}{F_2} = \frac{b \cdot h}{(b + 2 \cdot t) \cdot h} = \frac{1}{1 + 2t/b}$$

or

$$\frac{F_1}{F_2} = \frac{1}{1 + 2t/W \cdot W/b}$$

If this expression is introduced in equation (3), the final formula is obtained as:

$$K = \left[\left(\frac{2 \cdot t/W \cdot W/b}{1 + 2 \cdot t/W \cdot W/b} \right)^2 + \left(\frac{0.74 \cdot t/W \cdot W/b}{1 + 1.26 \cdot t/W \cdot Wb} \right)^2 \right] \qquad (4)$$

This is the loss coefficient for an expansion followed by a contraction. The equation is valid only when the distance between cross section variations is large as compared to the magnitude of cross section variation; i.e., only when t/W is small.

Abb. 34. Maßbezeichnung für die Nischen

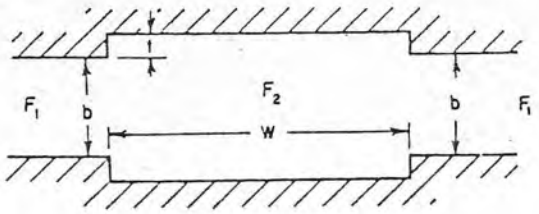

Figure 34. - Definition sketch for the slots.

If the distance between the expansion and the contraction is decreased, a point is reached at which the cross section variations have contrasting effects. This distance corresponds to a definite value of t/W and is designated here as critical depth ratio.

For small distance, i.e., large values of t/W, the region of slot flow begins. In this range, the loss is due to flow conditions in the slot and equation (4), therefore, does not hold.

Moreover, in cases where the magnitude of cross section variation is small as compared to the size of inlet cross section; i.e., when t/b is small, it is assumed that the effect of flow processes in one slot upon the flow processes in the opposite slot can be neglected. This is mathematically expressed by:

$$t/b \ll 1 \text{ or } t/W \cdot W/b \ll 1$$

With this assumption, one can conclude that for various length ratios W/b in the slots with the same depth ratios of t/W, similar flow processes are present. When, therefore, a given depth ratio corresponds to a given flow condition, the critical depth ratio has a constant value. The reason for this is that the critical depth ratio is defined as that depth ratio at which the flow from the expansion first begins to affect the flow at the contraction. Hence, there is only one depth ratio for which a definite flow condition occurs. The experiments showed that at a length ratio of W/b = 2.0, the critical depth ratio was 0.05. Since the condition t/W x W/b $\ll$ 1 is hereby fulfilled, it may be assumed that t/W = 0.05 is the value for critical depth ratios at all length ratios of W/b $\leq$ 2.0.

The critical depth ratio t/W = 0.05 can be taken as limiting value. For depth ratios smaller than t/W = 0.05, the loss is caused by an expansion and a contraction can be obtained from equation (4). On the other hand, for depth ratios larger than t/W = 0.05, the loss depends upon the slot ratios present. These losses have to be experimentally determined since completely theoretical treatment of these complicated flow processes in the slots is not yet possible.

Under the condition that:

a. For depth ratios longer than t/W = 0.05, the loss is determined only by flow conditions in the slots; and

b. In the slots with various length ratios, the flow conditions are similar at same depth ratios, it can be assumed that the ratio of loss for two different depth ratios is constant.

If, therefore, for a length ratio W/b = 2.0, the loss at t/W = 0.125 has a 1.6 times larger value than at t/W = 0.20, then the loss ratio is also the same for a length ratio W/b = 1.0 also. It follows that the slot loss coefficient for two arbitrary curves of constant length ratios are in a constant ratio to each other. If, therefore, at a depth ratio of t/W = 0.25, for a longitudinal ratio of W/b = 1.0, the loss coefficient is one-third of the loss coefficient for W/b = 2.0, the same loss ratio also exists for every other depth ratio.

The loss coefficients for various depth ratios can only be determined by experiments with a constant length ratio. From the experimentally obtained values, the loss coefficients for other length ratios are determined by a constant factor. The numerical determination of this factor (L) is possible by means of equation (4) since at critical depth ratio, the loss coefficient for arbitrary length ratios W/b can be determined.

Actually, the critical depth ratio is the unique depth ratio in the region of slot flow for which the loss can be expressed as a function of W/b by one equation.

The length ratio factor L is defined as:

$$L = \frac{K_b}{K_a} \qquad (5)$$

where, K_b is the loss coefficient for an arbitrary length ratio
K_a is the coefficient for a reference length ratio.

If the values of K_a and K_b, determined from equation (4) for critical depth ratio t/W = 0.05 and the reference length ratio W/b = 1.0 are substituted in equation (5), one obtains for L:

$$L = \frac{\left(\frac{0.10 \cdot W/b}{1 + 0.10 \cdot W/b}\right)^2 + \left(\frac{0.037 \cdot W/b}{1 + 0.063 \cdot W/b}\right)^2}{0.00947} \qquad (6)$$

According to previous discussion, therefore, the general form of slot loss coefficient can be represented by two curves. The first curve shows the flow loss coefficient depending upon depth ratio t/W for constant reference length ratio W/b = 1.0 (fig. 35). The second curve is derived from equation (6) and yields a factor with which the slot loss coefficient determined from figure 35 has to be multiplied. Thus, one obtains the slot loss coefficient for arbitrary length ratios (fig. 36). In figure 35, a comparison has been made between the experimental curve for length ratios W/b = 2.0 and 0.5 and the shape of reference curve. In this comparison, the ordinates of the experimental point are multiplied with the reciprocal value of corresponding factors. Theoretially, the curves have to overlap. Since the deviations are very small, there is good agreement with the theory. Furthermore, it is obvious with sufficient certainty that the mutual affect of flow conditions in opposite slots can be ignored for $t/W \cdot W/b \leq 1$ as compared with $t/W \cdot W/b \ll 1$,

The use of these curves can be illustrated with the following example:

The problem is to determine the loss caused by gate slots in a channel 2.0 m wide and 4.0 m height if the mean velocity in the channel is 5 m/s. The slots lie opposite each other and have a length of 50 cm and a depth of 20 cm.

The slot relation is

$$t/W = \frac{20}{50} = 0.40$$

From figure 35, a slot loss coefficient is 0.030 when the length ratio is W/b = 1.0. The actual length ratio, however, is:

$$W/b = \frac{0.5}{2.0} = 0.25$$

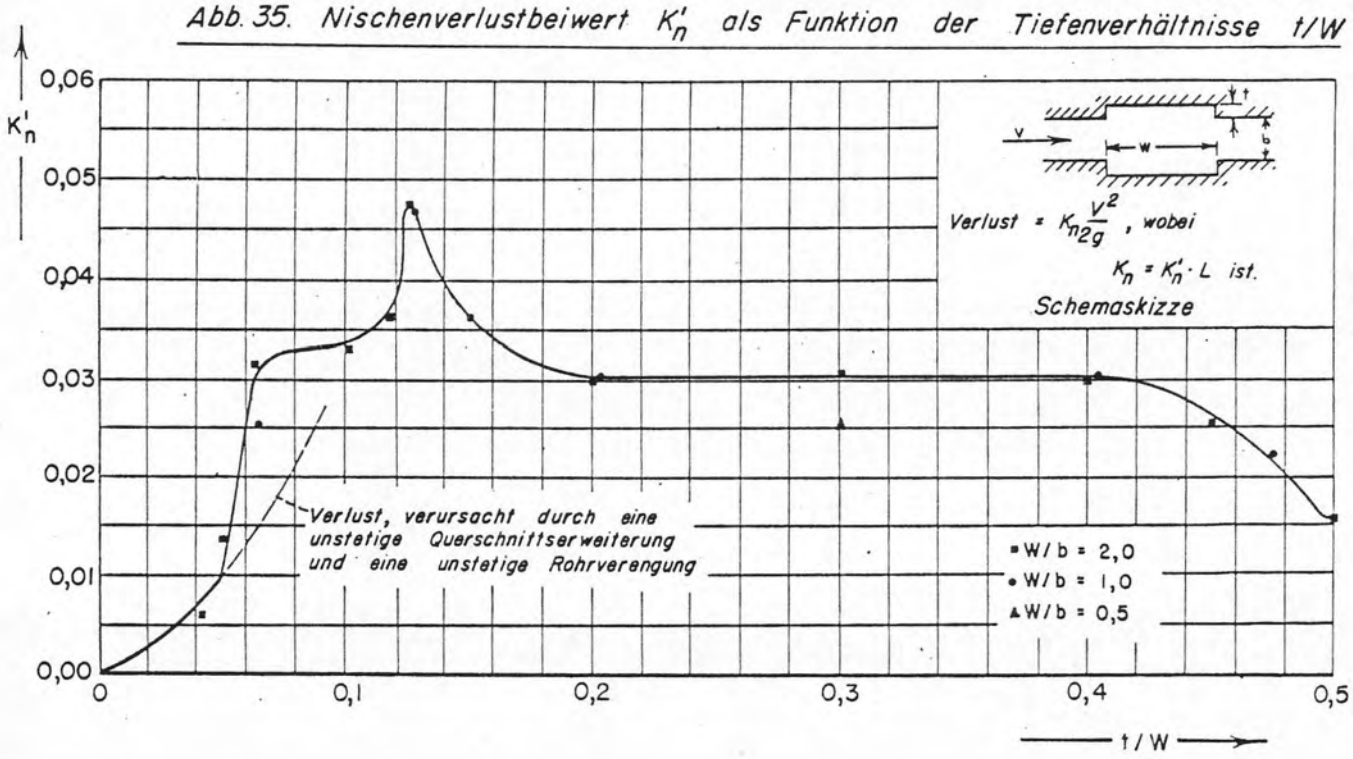

Figure 35. - Slot loss coefficient K_n as a function of depth ratio t/W.

Abb. 36. Längenverhältnisfaktor L als Funktion der Längenverhältnisse W/b

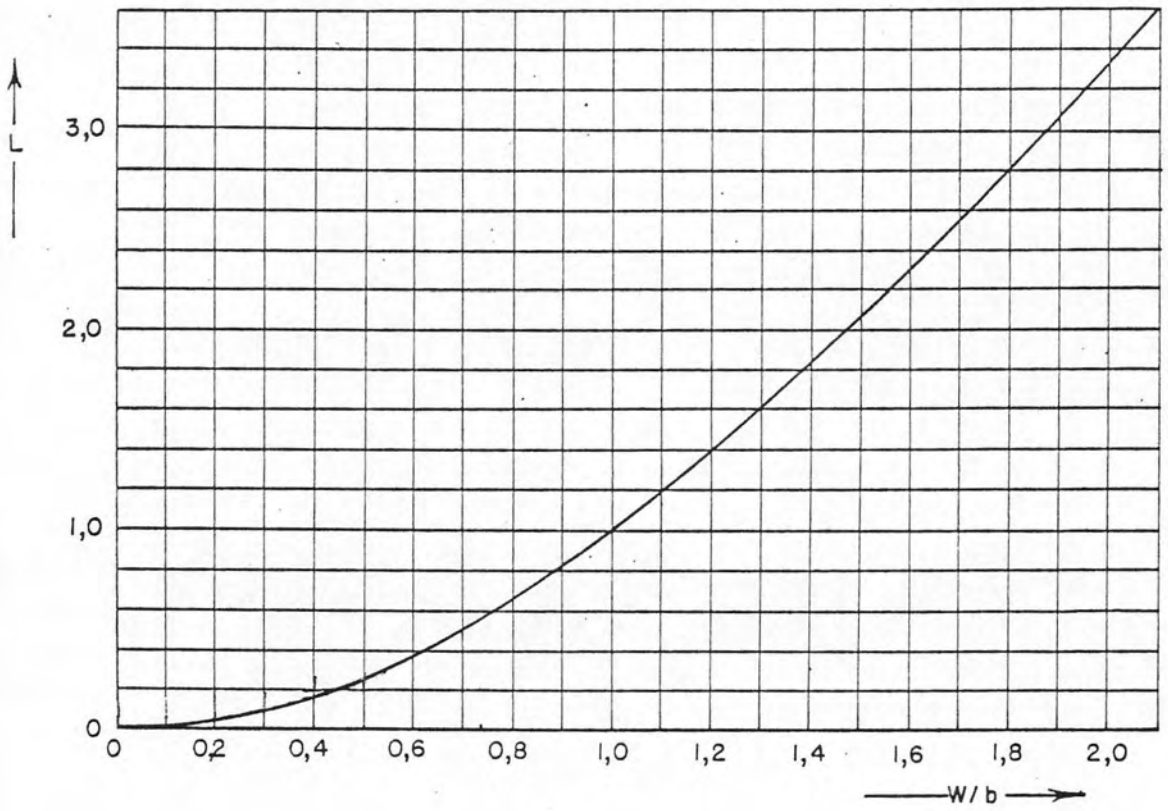

Figure 36. - Length ratio factor L as a function of length ratio W/b.

From figure 36, the length ratio factor L is 0.06. Hence, the slot loss coefficient for this slot ratio is:

$$K_N = 0.06 \cdot 0.030 = 0.0018$$

The mean velocity in the conduit is:

$$\frac{V^2}{2g} = \frac{25}{19.62} = 1.275 \text{ m}$$

Hence the loss due to gate slots is:

$$h_{loss} = K_N \frac{V^2}{2g} = 0.0018 \cdot 1.275 = 2.3 \text{ mm}$$

V. Effects of Changes Upon the Slots

A. Inserts

It has been found that inserts in the slots act to shorten slot lengths and decrease slot depths. In the inserts studied, the slot ratios without inserts were t/W = 0.20 and W/b = 1.00. Based on losses, the slot ratios with inserts are values of t/W = 0.127 and W/b = 0.85. The double action of shortening of length and decrease of depth of the slot is also visible in the flow condition. This double effect was, e.g., clearly seen in the flow condition in a partial model of a slot for a lock gate which was recently studied in the Institute of Hydromechanics, Technical University, Karlsruhe [13] (fig. 37). The effective dimensions of this slot with inserts are obviously the length of the insert and the depth of the wall up to the insert (compare this flow diagram with that of sections III.4.c to f, fig. 33).

Abb. 37. Schutznische in einer Schleuse [13]

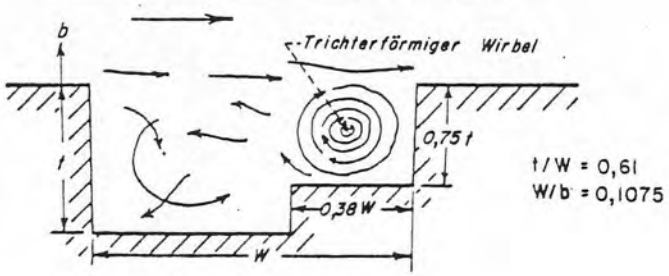

Figure 37. - Gate slot in a lock [13].

Abb. 38. Abwandlungen der rechteckigen Nischenform [12]

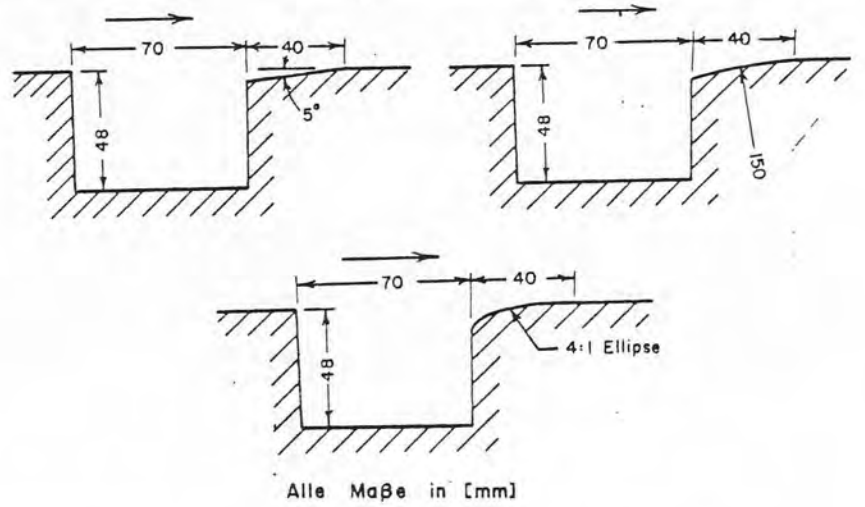

Figure 38. - Changes of rectangular slots [12].

B. Slots with downstream sloping edges

In practice, one frequently finds slots with sloping and elliptically rounded edges in order to reduce the danger of cavitation by this shape. The main effect of inclination and rounding is a reduction of flow constriction downstream of the slot so that the losses are perhaps smaller. In the form studies, the loss was 73 percent of that which was obtained for a slot without the slope. Tillmann [12] has found that the loss with a slope of -5° is equal to 86 percent, with a rounding of radius 150 mm is 72 percent and with an elliptic rounding of 4:1, it is 89 percent of the loss without slope (fig. 38). These examples give criterion for the magnitude for the change of losses which is caused by this type of slot forms.

VI. Summary

Slots are very frequently installed in the walls of channels and rectangular pipes as supports for stoplogs or gates. These slots produce an energy loss which has to be taken into consideration when measuring the efficiency of a turbine. Moreover, a knowledge of flow conditions in the slots is desirable since the turbulence occurring in the slot can damage the gate hoisting chains.

The study of flow in a slot led to the development of a semiempirical method for the determination of loss coefficients for arbitrary slot ratios. Moreover, the loss coefficients for modified slots, for instance, one with inserts and another with downstream sloping edges were also determined.

The flow conditions for various slot ratios have been systematically studied. It has been found that within given ranges of the ratio of slot depth to slot length, characteristic flow conditions occur. Moreover, the pattern of loss coefficient curves at various slot ratios has been explained on the basis of the flow conditions in the slots.

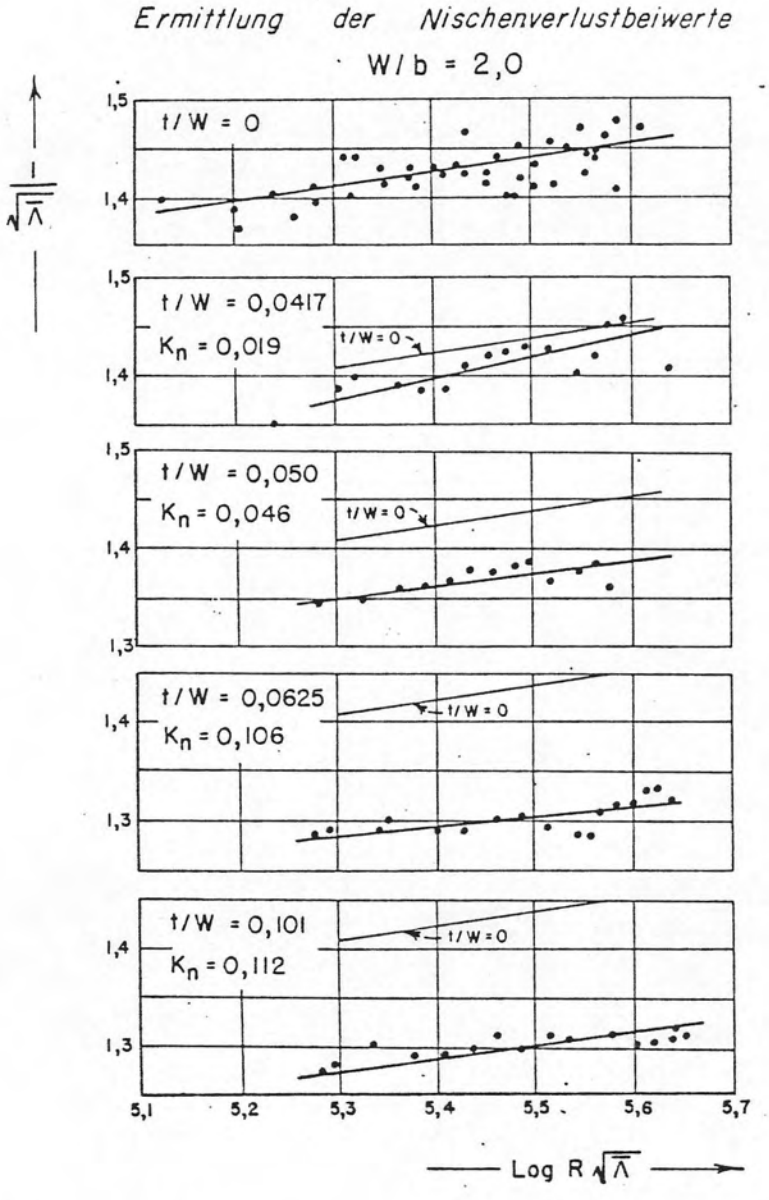

Appendix 1, Plate 1. - Determination of slot loss coefficient.

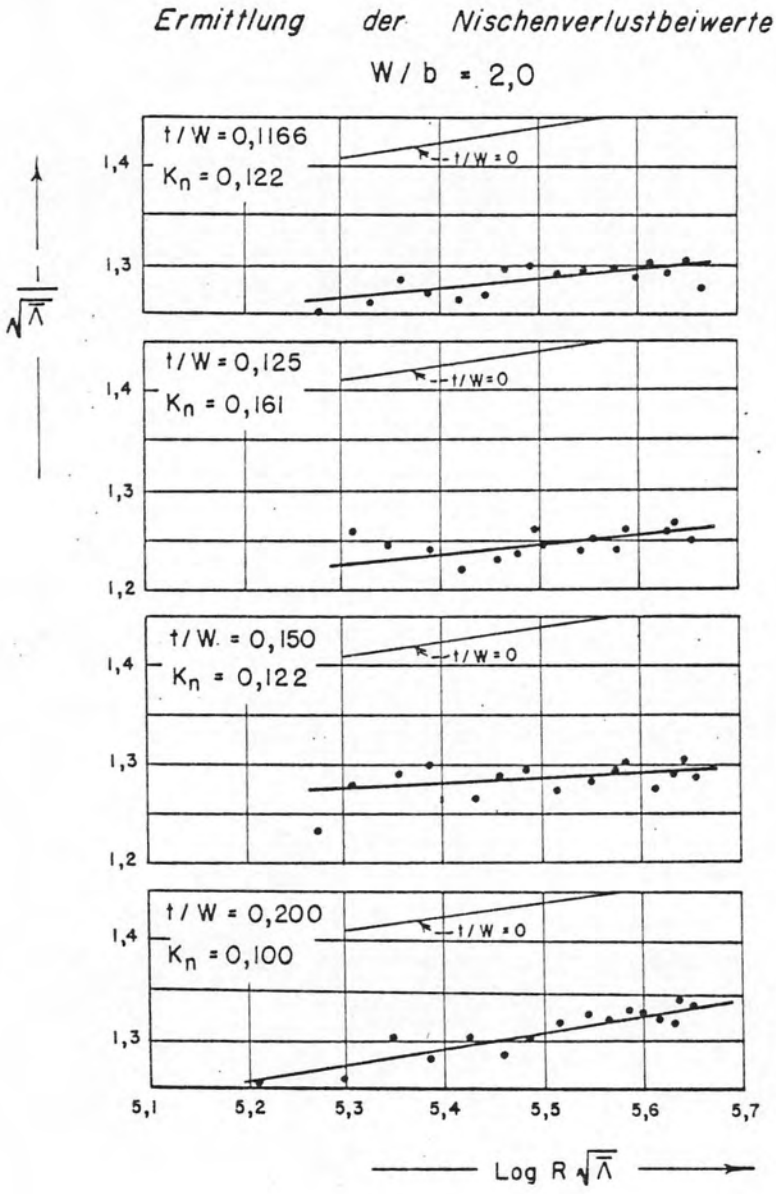

Appendix 1, Plate 2. - Determination of slot loss coefficient W/b = 2.0.

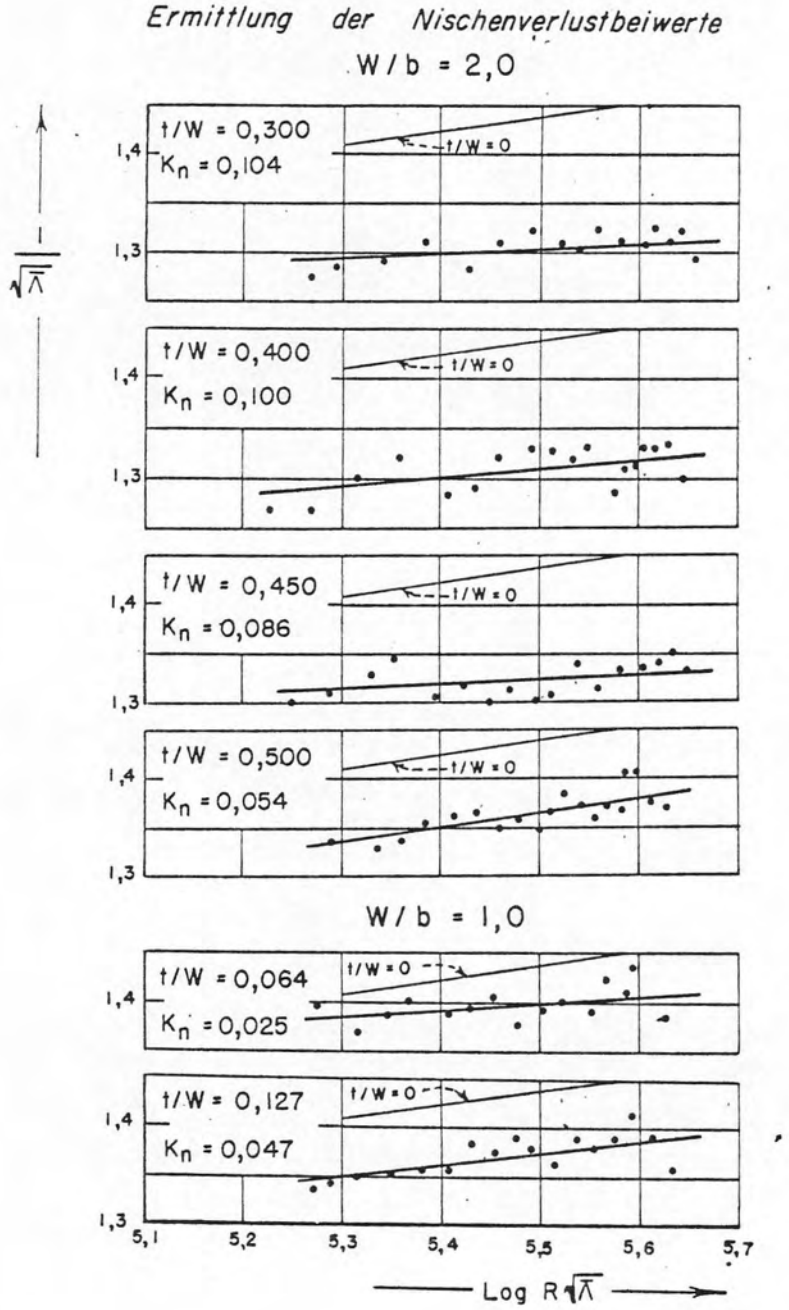

Appendix 1, Plate 3. - Determination of slot loss coefficient W/b = 2.0.

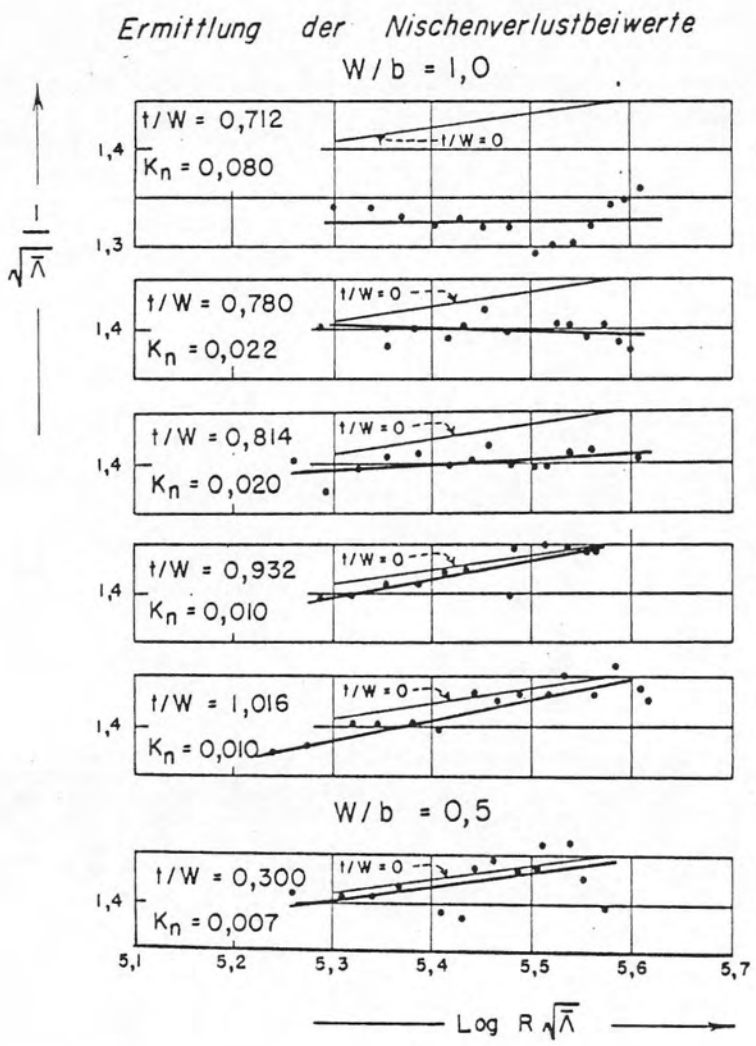

Appendix 1, Plate 4. - Determination of slot loss coefficient W/b = 1.0.

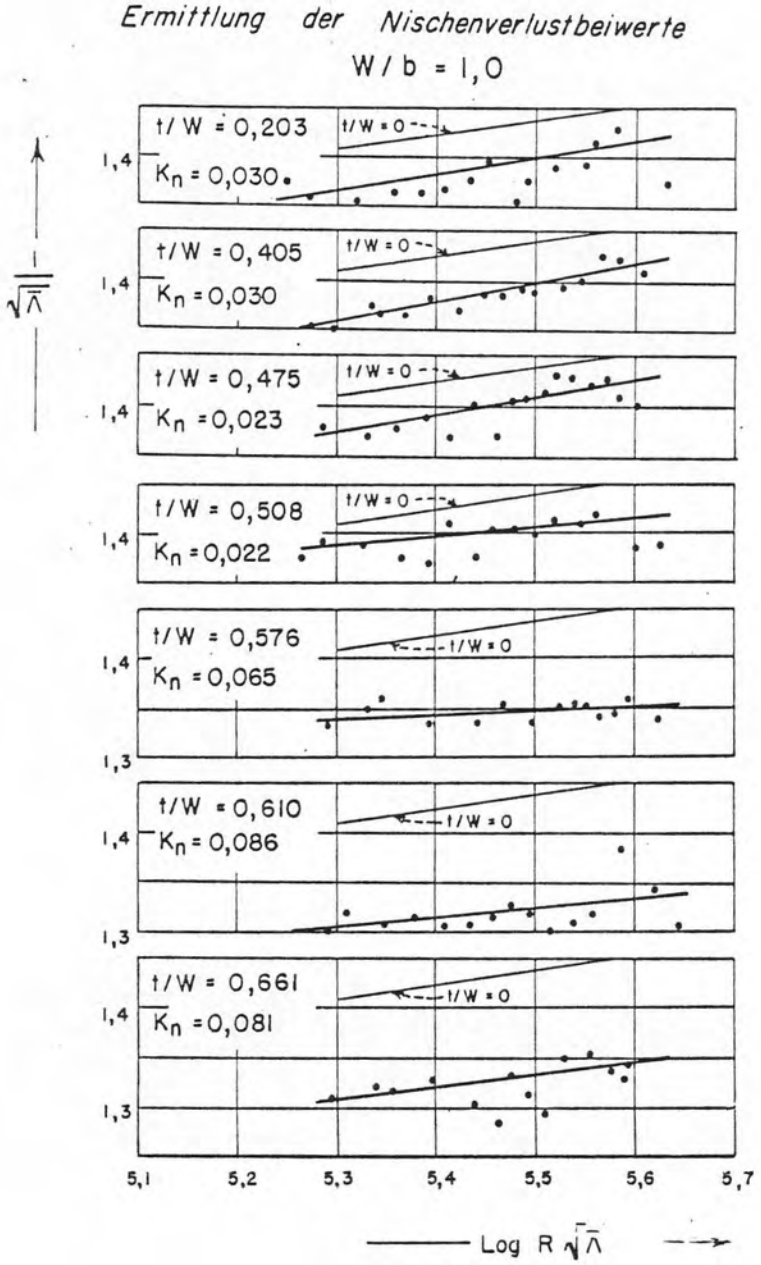

Appendix 1, Plate 5. - Determination of slot loss coefficient W/b = 1.0.

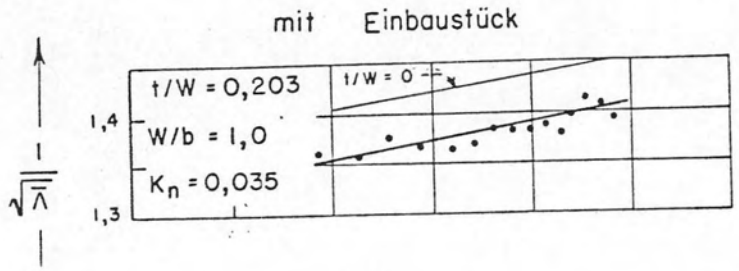

Appendix 1, Plate 6. - Determination of slot loss with inserts.

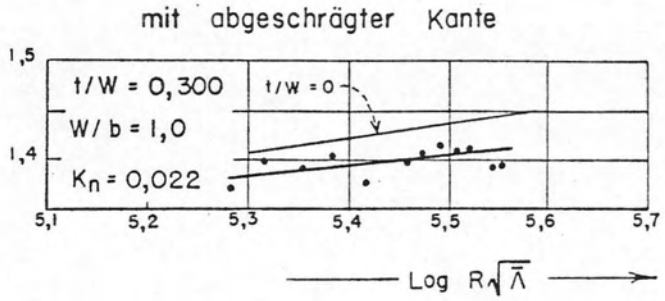

Appendix 1, Plate 6. - Determination of slot loss with sloping edge.